UNIVERSIDAD DE INVESTIGACIÓN DE TECNOLOGÍA EXPERIMENTAL YACHAY

Escuela de Ciencias Químicas e Ingenieria

TÍTULO: Atmospheric deposition in natural and anthropized environments in the north of Ecuador

Trabajo de integración curricular presentado como requisito para la obtención del título de Químico (a)

Autor:

Tugumbango Morales Jhoana Alexandra

Tutor:

MSc. Marta López

Urcuquí, Marzo 2020

Urcuquí, 27 de febrero de 2020

SECRETARÍA GENERAL
(Vicerrectorado Académico/Cancillería)
ESCUELA DE CIENCIAS QUÍMICAS E INGENIERÍA
CARRERA DE QUÍMICA
ACTA DE DEFENSA No. UITEY-CHE-2020-00004-AD

En la ciudad de San Miguel de Urcuquí, Provincia de Imbabura, a los 27 días del mes de febrero de 2020, a las 10:00 horas, en el Aula CHA-01 de la Universidad de Investigación de Tecnología Experimental Yachay y ante el Tribunal Calificador, integrado por los docentes:

Presidente Tribunal de Defensa	Dra. HIDALGO BONILLA, SANDRA PATRICIA , Ph.D.
Miembro No Tutor	Dr. SAUCEDO VAZQUEZ, JUAN PABLO , Ph.D.
Tutor	Mgs. LOPEZ ALCAÑIZ, MARTA

Se presenta el(la) señor(ita) estudiante **TUGUMBANGO MORALES, JHOANA ALEXANDRA**, con cédula de identidad No. **1004123434**, de la **ESCUELA DE CIENCIAS QUÍMICAS E INGENIERÍA**, de la Carrera de **QUÍMICA**, aprobada por el Consejo de Educación Superior (CES), mediante Resolución **RPC-SO-39-No.456-2014**, con el objeto de rendir la sustentación de su trabajo de titulación denominado: **Atmospheric deposition in natural and anthropized environments in the north of Ecuador**, previa a la obtención del título de **QUÍMICO/A**.

El citado trabajo de titulación, fue debidamente aprobado por el(los) docente(s):

Tutor	Mgs. LOPEZ ALCAÑIZ, MARTA
Co - Tutor	Dr. MAKOWSKI , KAMIL , Ph.D.

Y recibió las observaciones de los otros miembros del Tribunal Calificador, las mismas que han sido incorporadas por el(la) estudiante.

Previamente cumplidos los requisitos legales y reglamentarios, el trabajo de titulación fue sustentado por el(la) estudiante y examinado por los miembros del Tribunal Calificador. Escuchada la sustentación del trabajo de titulación, que integró la exposición de el(la) estudiante sobre el contenido de la misma y las preguntas formuladas por los miembros del Tribunal, se califica la sustentación del trabajo de titulación con las siguientes calificaciones:

Tipo	Docente	Calificación
Presidente Tribunal De Defensa	Dra. HIDALGO BONILLA, SANDRA PATRICIA , Ph.D.	9,6
Miembro Tribunal De Defensa	Dr. SAUCEDO VAZQUEZ, JUAN PABLO , Ph.D.	9,2
Tutor	Mgs. LOPEZ ALCAÑIZ, MARTA	9,9

Lo que da un promedio de: **9.6 (Nueve punto Seis)**, sobre 10 (diez), equivalente a: **APROBADO**

Para constancia de lo actuado, firman los miembros del Tribunal Calificador, el/la estudiante y el/la secretario ad-hoc.

TUGUMBANGO MORALES, JHOANA ALEXANDRA
Estudiante

Sandra P. Hidalgo B.

Dra. HIDALGO BONILLA, SANDRA PATRICIA , Ph.D.
Presidente Tribunal de Defensa

Mgs. LOPEZ ALCAÑIZ, MARTA
Tutor

UNIVERSIDAD DE INVESTIGACIÓN DE TECNOLOGÍA EXPERIMENTAL YACHAY
YACHAY TECH
ESCUELA DE CIENCIAS QUÍMICAS E INGENIERÍA

Dr. SAUCEDO VAZQUEZ, JUAN PABLO , Ph.D.
Miembro No Tutor

ESCOBAR LANDAZURI, ANA MARIA
Secretario Ad-hoc

AUTORÍA

Yo, **JHOANA ALEXANDRA TUGUMBANGO MORALES**, con cédula de identidad 1004123434, declaro que las ideas, juicios, valoraciones, interpretaciones, consultas bibliográficas, definiciones y conceptualizaciones expuestas en el presente trabajo; así cómo, los procedimientos y herramientas utilizadas en la investigación, son de absoluta responsabilidad de el/la autora (a) del trabajo de integración curricular. Así mismo, me acojo a los reglamentos internos de la Universidad de Investigación de Tecnología Experimental Yachay.

Urcuquí, Marzo - 2020.

Nombres y Apellidos: Jhoana Alexandra Tugumbango Morales

CI: 1004123434

AUTORIZACIÓN DE PUBLICACIÓN

Yo, **JHOANA ALEXANDRA TUGUMBANGO MORALES,** con cédula de identidad 1004123434, cedo a la Universidad de Tecnología Experimental Yachay, los derechos de publicación de la presente obra, sin que deba haber un reconocimiento económico por este concepto. Declaro además que el texto del presente trabajo de titulación no podrá ser cedido a ninguna empresa editorial para su publicación u otros fines, sin contar previamente con la autorización escrita de la Universidad.

Asimismo, autorizo a la Universidad que realice la digitalización y publicación de este trabajo de integración curricular en el repositorio virtual, de conformidad a lo dispuesto en el Art. 144 de la Ley Orgánica de Educación Superior

Urcuquí, Marzo - 2020.

Jhoana

Nombres y Apellidos: Jhoana Alexandra Tugumbango Morales
CI: 1004123434

Dedicatoria

Dedico este trabajo de investigación principalmente a Dios, por ser el inspirador y la fortaleza para continuar en este proceso de obtener uno de los deseos más deseados.

A mi familia, especialmente a mi madre por su amor, trabajo y sacrificio en todos estos años, gracias a ti, logré llegar aquí. Estoy infinitamente agradecido por los consejos, valores y principios que me han sido inculcados.

Jhoana Alexandra Tugumbango Morales

Agradecimiento

Me gustaría expresar mi sincero y profundo agradecimiento a mis asesores de tesis, MSc. Marta López Alcañiz y el Dr. Kamil Makowski por la ayuda, orientación y sobre todo la paciencia que me brindaron para la realización de esta tesis, por su apoyo y amistad que me permitieron aprender mucho más de lo que estudié en el proyecto.

Un sincero agradecimiento al Dr. Jorge Pey y a todo su grupo de trabajo por su colaboración en el desarrollo experimental del trabajo de tesis.

Agradezco a los maestros de la Facultad de Ciencias Químicas e Ingeniería de la Universidad Tecnológica de Yachay, por compartir sus conocimientos a lo largo de la carrera universitaria. Que con su sabiduría, conocimiento y apoyo, me motivaron a desarrollarme como persona y profesional.

Agradezco a mi familia por su apoyo incondicional en todo momento.

Jhoana Alexandra Tugumbango Morales

Resumen

Los aerosoles atmosféricos, una vez que se completa su ciclo en la atmósfera, se transfieren a las superficies de la Tierra a través de deposición húmeda y seca. El impacto generado por la deposición es relevante ya que podría desequilibrar la composición del suelo y convertirse en una fuente de contaminación para el suelo, el agua y los ecosistemas terrestres. La presencia de aerosoles en el aire en sí está correlacionada con problemas de salud, principalmente del sistema respiratorio y es necesario controlarla. La presencia de estos contaminantes del aire ocurre tanto por procesos naturales como por actividades antrópicas. Este proyecto tiene como objetivo evaluar la caracterización atmosférica del proceso de deposición en la provincia de Imbabura en tres lugares estratégicamente elegidos teniendo en cuenta los entornos naturales y antrópicos, así como diferentes altitudes. Estos lugares son Ibarra, Yachay y San Antonio de Ibarra. Las muestras se recolectaron mensualmente durante un año a partir de noviembre de 2018.Estos se filtraron y analizaron tanto la composición soluble como la insoluble de las muestras de precipitación. El material insoluble se analizó mediante fluorescencia de rayos X, mientras que el material soluble como los aniones se determinó mediante cromatografía iónica. Los cationes se obtuvieron mediante un analizador de flujo continuo y los metales traza se analizaron mediante espectrometría de emisión atómica de plasma acoplado inductivamente. A través de los resultados obtenidos, fue posible determinar las diferentes fuentes de contaminación en los lugares analizados y las concentraciones de compuestos que podrían ser perjudiciales para la salud.

Palabras clave:
Atmósfera, aerosoles, precipitación, iones, antropogénico, Imbabura, Ecuador.

Abstract

Atmospheric aerosols, once their cycle in the atmosphere is completed, are transferred to Earth's surfaces through wet and dry deposition. The impact generated by the deposition is relevant since it could imbalance the composition of the soil and become a source of pollution for the soil, water and terrestrial ecosystems. The presence of aerosols in air itself is correlated to health problems mainly respiratory system and need to be monitored. The presence of these air pollutants occurs both by natural processes and by anthropic activities. This project aims to assess the atmospheric characterization of the deposition process in the province of Imbabura in three strategically chosen places taking into account natural and anthropic environments as well as different altitudes. These locations are Ibarra, Yachay and San Antonio de Ibarra. Samples were collected monthly for one year from November 2018. These were filtered and analyzed both the soluble and insoluble composition of the precipitation samples. Insoluble material was analyzed by X-ray fluorescence while soluble material such as Anions were determined by Ion Chromatography cations were obtained by Continuous Flow Analyzer and trace metals were analyzed by Inductively coupled plasma atomic emission spectrometry. Through the results obtained, it was possible to determine the different sources of contamination in the analyzed places and the concentrations of compounds that could be harmful to health.

Key Words:

Atmosphere, aerosols, precipitation, ions, anthropogenic, Imbabura, Ecuador.

CONTENT

1 TITLE

Atmospheric deposition in natural and anthropized environments in the north of Ecuador

2 INTRODUCTION-JUSTIFICACION

2.1 ATMOSPHERE

The atmosphere is composed of gases, solid and liquid particles in suspension attracted by the Earth's gravity. The atmosphere is approximately 10,000 km thick and distributed in layers called exosphere, thermosphere, mesosphere, stratosphere and troposphere [1]. The troposphere is the lowest layer of the Earth's atmosphere that forms from the Earth's surface to the tropopause in it is approximately 80 % mass of the entire atmosphere and almost all the water vapor that allows the formation of clouds and rain [2].

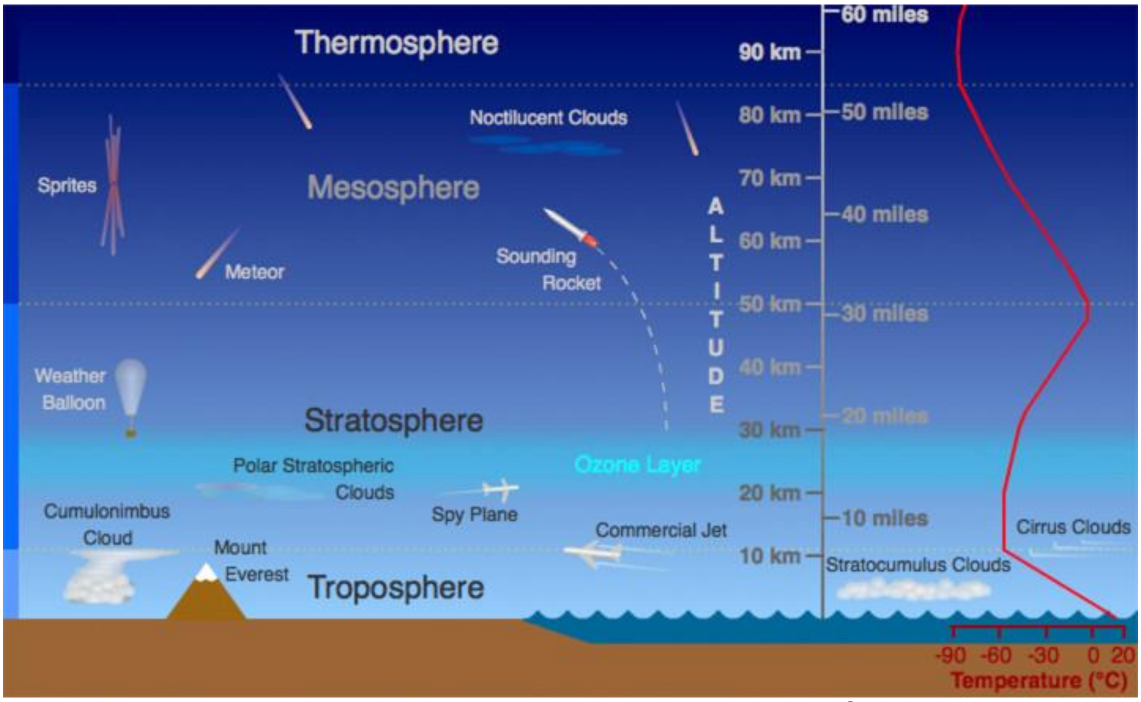

Figure 1. Layers of Earth's Atmosphere. Reproduced from [3].

The main sources of air pollution are natural and anthropogenic emissions. Among the most important sources are the emission of fossil combustion, forest fires, volcanic eruptions and decomposition of organic matter. In the case of anthropogenic emissions are industrial processes, productions of vehicular cement, construction, production of biocides and pesticides and mining activities [4].

2.2 ATMOSPHERIC AEROSOLS

Aerosols are small particles that are suspended in the atmosphere; there is a great variety of them that differ in their sizes, morphologies and chemical compositions. It’s can use as nucleation processes that produce rainfall or interact with radiation [5] [6].

2.2.1 TYPES OF ATMOSPHERIC AEROSOLS

The particles emitted directly in the atmosphere are called primary particles while those that were formed in the atmosphere through the conversion of gas to particle are called secondary particles [7]. Particles of primary origin come from both natural and anthropogenic sources such as fossil fuels, use of pesticides and inadequate treatment with industrial effluents [8]. While, the secondary components can be generated by a new particle formation, particle gas partition or heterogeneous or multi-phase reactions. The particles that are generally found in the atmosphere are the particulate material such as sulfate, nitrate, carbon monoxide ammonium, sea salt, mineral dust, organic compounds and black or elemental carbon as well as the presence of biogenic particles as remains of plants and animals [9].

2.2.2 SIZE OF ATMOSPHERIC AEROSOLS

The particles can be classified as a coarse, fine and ultrafine fraction. The coarse fraction is composed of particles whose diameter is between 2.5 and 10 µm ($PM_{2.5\text{-}10}$). The fine fraction is composed of particles whose diameter is less than 2.5 µm ($PM_{2.5}$) and the ultrafine fraction refers to particles smaller than 0.1 µm. Secondary aerosols are usually in the fine mode, while primary particles are mostly coarse [10].

The National Institute of Ecology and Climate Change of Mexico (INECC) presented a methodological guide for the estimation of $PM_{2.5}$ emissions and it mentions research in which it has been possible to characterize the particulate material (PM) as shown in the Figure 2.

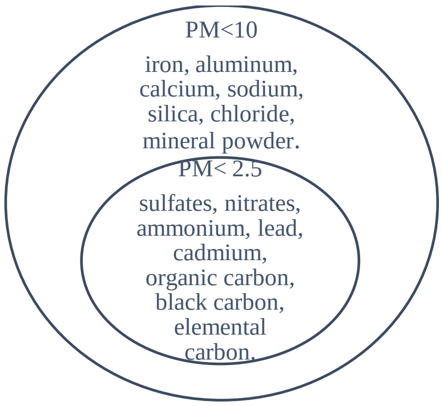

Figure 2. Particle material characterization. Reproduced from[10]*.*

It is worth to mention that elemental carbon is one in which only carbon is found in its composition while black carbon is an internal mixture of elements and gives soot its black color. Both are the result of incomplete combustion of fossil fuels, biofuels and biomass [11] [12].

While the process of particle formation can be summarized in the Table 1.

	Types of Particles		
	Ultrafine ($PM_{0.1}$)	**Fine ($\leq_{2.5}$)**	**Coarse ($PM_{2.5}$-PM_{10})**
Training Processes	Nucleation of atmospheric gases, including H_2SO_4, NH_3 and some organic compounds. Condensation of gases.	Condensation of gases. Coagulation of small particles Gas reaction in or on particles. Evaporation of mist and drops of water in which the gases have dissolved and reacted.	Mechanical processes (pressing, grinding, abrasion, breaking solids / drops) Aerosol Evaporation Powder suspension Gas reaction in or on particles

Table 1. Formation process of particulate matter. Reproduced from [10].

2.3 WAYS OF DEPOSITION.

All these type of particles in the atmosphere reach the surface of the earth from wet and dry deposition [7]. Wet deposition uses rain, snow or mist droplets as a means of transport to be incorporated into the surface of the Earth while dry deposition is generated due to the effect of gravity or wind. The analysis of samples from dry deposition is more complicated because it is more difficult to collect samples from the soil surface and to distinguish if it was a product of the deposition or composition of the soil [13]. The impact generated by the deposition can be relevant since it could unbalance the composition of the soil and become a source of contamination for soil, water and terrestrial ecosystems [8].

2.3.1 PRECIPITATION

The precipitation process begins with evaporation in which water passes from a liquid to a gaseous state and rises into the atmosphere like a gas. As the saturated air rises, it cools and adheres to aerosols such as dust particles, salts, seeds or smoke in the atmosphere becoming condensation nuclei. As water vapor condenses, cloud formation begins, they heat up and gain weight until it falls to the ground like rain [14].

In 2017, in Ecuador, an exhaustive analysis of precipitation data has been carried out in all the monitors networks that National Institute of Meteorology and Hydrology (INAMHI) has corresponding to 2013. Therefore, it has been concluded that there are different precipitation trends in the 3 different regions of Ecuador. In the Sierra, the months of January to May are where the greatest number of rainfall occurs, while in the months of June to August the rainfall is considerably reduced. In the Costa region the lack of rain maintained since June until November. While in the Oriente region it is where the greatest number of rainfalls occurs throughout the year [15].

Acid rain

Acid rain is the precipitation in which a mixture of sulfuric and nitric acids is mainly combined [16]. The H_2SO_4 and HNO_3 that are generated because SO_2 and NO_2 oxidize to form SO_3 and NO_3^- and being very reactive, react with water and form H_2SO_4 and HNO_3 respectively. SO_2 and NO_x come from anthropogenic and natural sources of contamination [17]. For rainwater pH=5.6 is considered normal, below of this value is consider presence of acid rain. [18]. In this study the possible presence of acid rain in Imbabura will be determined from the concentration of NO_3^- and SO_4^{2-}.

Conductivity

Conductivity is the ionic ability to carry electrical current. In water, ions are responsible for transporting electricity. The SI unit for expressing conductivity is the Siemens per meter (S/m), measurement of electrical conductivity [19]. The conductivity shows the amount of dissolved matter in the water. It is gives a notion of the amount of ions in solution such as Cl^-, NO_3^-, SO_4^{2-}, PO_4^{3-}, Na^+, Mg^{2+} and Ca^{2+} [20]. It is important to consider the ranges of water conductivity values. Ultrapure water has a conductivity of 0.055 µS/cm, drinking water has a conductivity between (50 - 500) µS/cm and sea water 50000 µS/cm [21].

2.4 EFFECTS OF ATMOSPHERIC AEROSOLS

The effects of atmospheric aerosols are studied by the relationship that has with factors such as health, climate and ecosystems [22]. In the case of climate, aerosols can affect it through their interactions with radiation and clouds [13]. The particles affect the climate system by dispersing and absorbing solar radiation and can also act as cloud condensation nuclei (CCN) [23].

2.4.1 EFFECT OF AEROSOLS IN NATURAL ENVIRONMENTS

In some regions, the development of the ecosystems depends to a great extent on the deposition of the particles that are in the atmosphere since these can contribute as nutrients for the development of the vegetation. Although it can also have negative effects on agriculture since the presence of metal compounds can reduce the yield of crops [13]. The process in which atmospheric aerosols divert solar radiation can also affect the production of crops [24].

2.4.2 EFFECT OF AEROSOLS ON HEALTH

The World Health Organization (WHO) shows that in 2012, air pollution resulted in the death of 3.7 million people worldwide. The main diseases that were recorded were due to a cardio-vascular accident, chronic obstructive pulmonary, lung cancer, ischemic heart disease and acute respiratory infection [25].

When comparing 2012 and 2016, the increase in deaths from obstructive pulmonary disease was recorded from 11% to 18%. Respiratory diseases increased from 3% to 18%. Stroke increased from 40% to 58% while lung cancer deaths remained at 6% [26] [25]. In Spain it is estimated that 19,940 premature deaths per year related to air pollution [27]. Table 2 shows the common diseases that cause different pollutants.

Pollutants	Efects
PM_{10} and $PM_{2.5}$	Reduction of lung function: frequency of respiratory diseases. Aggravation of asthma and chronic bronchitis. Early death. Silicosis and asbestosis. Cold and asthma exacerbation. Chronic obstructive pulmonary disease. Exacerbation of chronic obstructive pulmonary disease.
CO	Headache, irritability, decreased auditory and visual perception. Interferes with the transport of O2 by hemoglobin.
Cd^{2+}, V and Pb^{2+}	Renal toxicity Higher frequency of arterial hypertension in the adult population.
Pb	Tubulopathy Anemia Replacement of Ca^{+2} in the bones causing decalcification
SO2	Irritation of eyes and mucous membranes. cardiovascular damage
NO2	Damage to liver, spleen and blood.

Table 2. Health effects of air pollutants. Reproduced from [28] [29] [30].

2.5 SOURCES OF AEROSOL PARTICLES

The main sources of atmospheric particles can be classified according to their formation origin as natural and anthropogenic. Natural atmospheric particles are found in greater composition in the atmosphere than anthropogenic but man-made sources represent a more significant threat in the short, medium and long term [31].

2.5.1 NATURAL SOURCES

Forest fires

Forest fires are a main source of smoke, SO_2 NO_2, ozone, particles, CO_2 and CO into the atmosphere [31]. In the same way solid or liquid suspended particles such as soot and other volatile organic substances. The size of these particles is in the range of PM_{10}, $PM_{2.5}$, PM_1 or even of a smaller diameter. All of these compounds can cause cardiovascular and respiratory problems [32]. Focusing on Ecuador in recent months, when study was carried out a series of fires natural and induced have been recorded that have largely affected the northern part of the country.

Secretary of Risk Management has registered that in 2019 the provinces that report the greatest number of forest fires were: Imbabura, Pichincha and Chimborazo. In the province of Imbabura, 182 fires had been recorded from July to August, being considered the second province with the highest fires after Pichincha in 2019 that has registered 203 fires. In addition, the report records a comparative analysis that shows that so far last year the number of forest fires that were generated in 2018 has already been exceeded. In the province of Imbabura, the most affected cantons have been Cotacachi, Otavalo , Ibarra and Urcuqui [33].

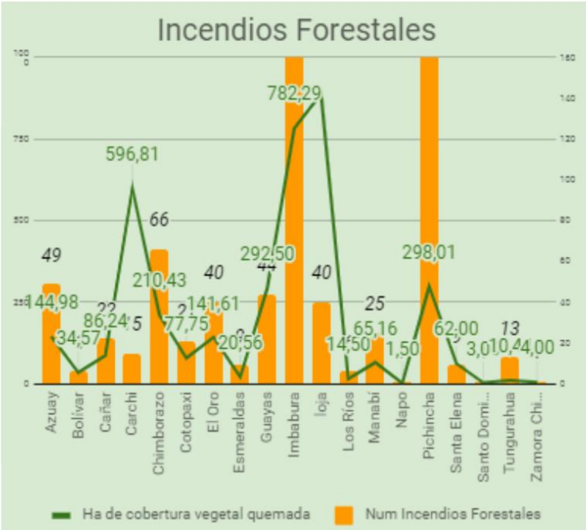

Figure 3. Forest fires presented in each of the provinces in Ecuador since 07/01/2019. Reproduced from [33].

Volcanic eruptions

During the eruptive processes, contaminating particles such as H_2O, CO_2, SO_2, HCl, HF, H_2, S_2, CO H_2S and SiF_4 are expelled [34]. El Reventador is considered one of the most active volcanoes in Ecuador. This volcano is located approximately 90 km from Quito, between the provinces of Napo and Sucumbíos. This volcano has registered eruptive processes in the months of June and August 2019. [35].

Decomposition of organic matter

This process involves the decomposition of animals and plants that are deposited in the soil as organic compounds. Decomposing plants and animals generate methane and hydrogen sulfide [31].

Source	Main Pollutants
Volcanoes	SO_x
Forest fires	CO_2, CO, NO_x
Dust storms	Particles
Decomposing plants	CH_4, H_2S
Swamps	Harmful Gases

Table 3. Main sources of aerosol particles. Reproduced from [31].

2.5.2 ANTHROPOGENIC SOURCES

Industrial Process

Industrial processes involve a series of activities that are carried out to transform the raw material and generate it into products necessary to improve and meet the needs of the public [36]. Industrialization such as cement production buildings and vehicular traffic can release toxic substances to the environment. Among the main industrial processes are:

Cement Production

In the cement refinery process, the main pollutants are SO_2, CO, NO_x and suspended particles. The cement production process is also linked to combustion processes releasing volatile organic compounds (VOCs) [37]. An investigation carried out at the National Institute of Environmental Engineering Research of India showed that Ca^{2+}, NO_3^-, SO_4^{2-}, As, Cd, Co, Cr, Cu, Fe, Mn, Ni, Pb and Zn^{2+} are the main elementary contents of raw materials. [38]. In the province of Imbabura, *Selva Alegre* Cement Company is the largest cement producer in the northern part of Ecuador. Also there are places where the cement is constantly produced, releasing particles in the air. In the Figure 4, we could see where are located, these are in all Imbabura province considering as important source of these elements.

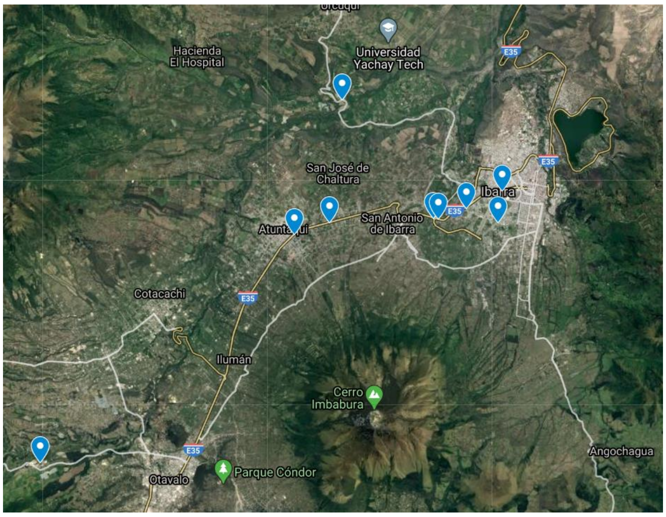

Figure 4. Location of places where the cement worked in Imbabura. Reproduced from [39].

Constructions, and Floor

Constructions and demolitions originate particles such as aluminum, silica, iron and calcium [10]. In the case of soils, soil erosion generates dust particles, and these are released into the atmosphere by factors such as water and climate [40].

Vehicular Traffic

Transport is the main emitter of pollutants such as CO_2 from soot ash and solid core particles of less than 10 nm to the atmosphere, so in highly urbanized areas there tends to be an excessive concentration of this gas. Emissions will depend on the vehicle's technology properties of fuels and lubricating oils [41].

In Ecuador, one of the main pollutants are transport due to the mechanical shortcomings that the majority of both public and private have [42]. An analysis by the National Transit Agency (ANT) show that in 2010 there were two million transport units and that until 2015 this value increase by 57% [43].

Table 4 shows a summary of the possible sources of emission of metals and ions detected in the atmosphere.

Metals and Ions	**State**	**Posible Source**

Fe	Fe_2O_3	Fossil fuels and diesel emissions and road dust [44]. Construction process, demolition by the use of cement [45].
P	P_2O_5	Phosphate fertilizers [46]. Wastewater [47].
Ca	CaO	Construction process, demolition by the use of cement. Contributed by lime [45]. Soil erosion
Al	Al_2O_3	Construction process, demolition by the use of cement, mineral element. [45].
K^+	K_2O	Construction process, demolition by the use of cement [45]. Soil erosion. Organic material. Fertile soil composition [48].
SO_4^{2-}		Volcanic emissions, production of cement or related materials [38]. Burnig of fossil fuels.
Ba	BaO	Barium is released into the air mainly by the production of paints, bricks, ceramics, glass and rubber. It is also issued in the processes of extraction, production of compounds derived from barium. Also during the combustion process of coal and oil. [49].
Cd		Cadmium is exposed to the air by extracting non-ferrous metals, it is also used in the manufacture and application of specially phosphate fertilizers, and finally it is also transmitted in the combustion and incineration processes of fossil fuels. [50].
V		Continental dust, marine aerosols and volcanic emissions. Industrial sources of vanadium are oil refineries and power plants that use fuel oil and coal rich in vanadium [51].
Zn	ZnS	Mining.
		Purification of zinc, lead and cadmium minerals, steel production, coal burning and waste burning [52].
Mg	MgO $MgSO_4$	Chemical composition of the majority of fertilizers since it generates the green color to the plants [53]. Carbonantes and marine salts
Na^+,Cl^-	NaCl	Marine aerosols.
Cu	$CuSO_4$	Agriculture (Plant diseases, such as mold). Water treatment Preservatives for wood, leather and fabrics [54]. Cement Production [38].

Table 4. Sources of emission of metals and ions detected in the atmosphere.

2.6 MONITORING OF AEROSOLS IN LATIN AMERICA

2.6.1 BOGOTA COLOMBIA

Bogota, capital of Colombia, a city with approximately 7.413 million inhabitants. At an average height of 2625 meters above sea level. Located in the center of Colombia. It has a territorial length of 33 km from north to south and 16 km from east to west [55].

Climatology

During 2018 on average it was reached at a temperature of 14.5 °C regarding this average, an increase of 0.4 to 0.7 °C was seen in the southwest and northwest of Bogotá. While in the rest of the city a slight decrease in temperature was measured. With respect to precipitation levels, the graph shows that the maximum precipitation levels are shown in the first half of the months from February to May that reach 140 mm and in the second half in the months of October and November. While in the remaining months levels below 140 mm were reached [56].

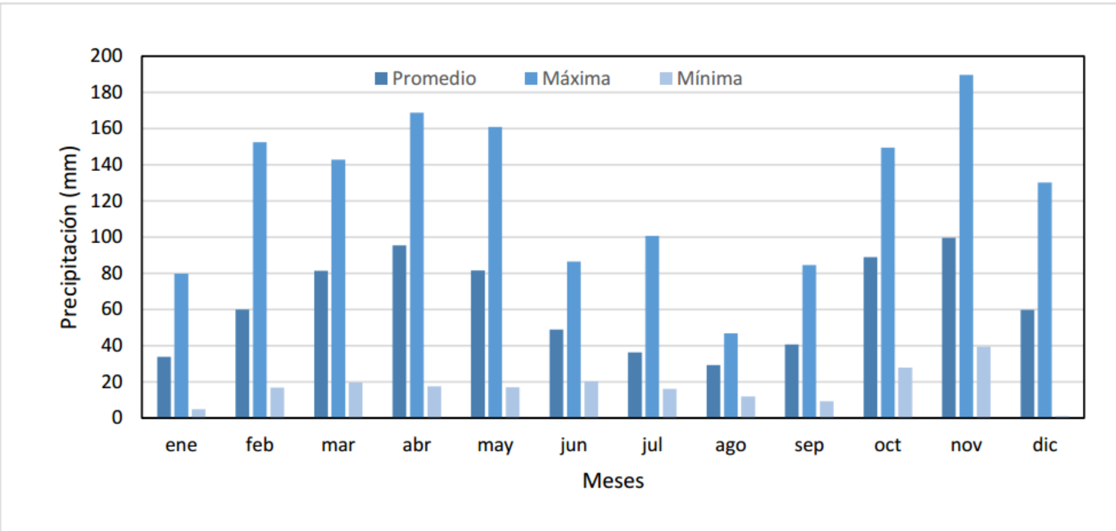

Figure 5. Amount of monthly precipitation in Bogota in 2018. Reproduced from [56].

Contamination Sources

A study carried out in 2017 by the University of Huelva identified that the main source of PM_{10} pollutions vehicular traffic because vehicle exhaust emissions and road dust emissions are the 50% of the mass of PM_{10}. Other sources of pollution also include the associated emissions of gasoline and diesel from vehicles, sources of combustion, industrial sources, forest fires, soil erosion and construction activities [57].

Air quality monitoring.

Air Quality Monitoring Network of Bogotá (RMCAB) reports annually on the state of air quality in the city. It has 11 stations located in different parts of the city. In the report issued in 2018, it shows that two of the stations located in Bogotá show values that exceed and are at the limit of the values allowed in the city. Carvajal-Sevillana (CSE) station located south of the town of Kennedy, considered an urban area, shows the most worrying data because it exceeds the allowed limit of 69 ug/m^3 vs 50 ug / m^3 allowed for PM10 emission. Kennedy station (KEN) located more to the center of the town of the same name registers a value of 50 ug/m^3 of PM_{10} emission [56].

A study conducted in 2010, tries to determine the chemical composition and particulate material in Bogota, showed the presence of high levels of Al, Si, Ca, Fe and elements with lower concentration such as Zn, Cu, Pb. Cations and anions were also determined as K^+, Na^+, $NH_4{}^+$, $Ca^{2+,}$ $SO_4{}^{2-}$, $NO_3{}^-$ [57]. These studies were conducted in two urban areas of the city of Bogotá. Figure 6 shows the concentrations of the elements detected in the air of Bogotá. The study associates the presence of Al, Si, Ca and Fe from mineral sources and Zn, Cu and Pb, to vehicular or industrial sources.

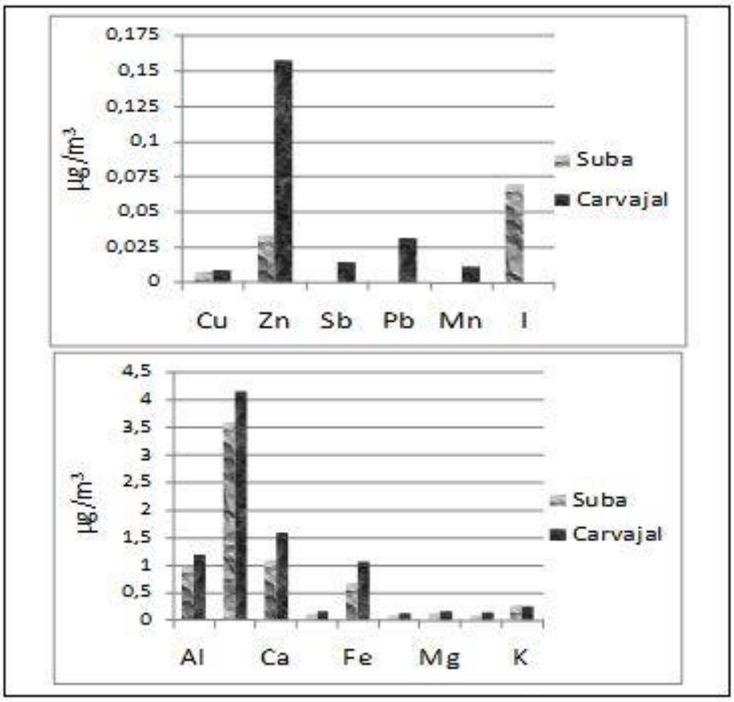

Figure 6. Concentration values of the elements found in Bogota. Reproduced from [57].

3 PROBLEM STAMENT

The process of deposition by both wet and dry roads has direct consequences that affect the environment of the ecosystem such as soil, water resources and the climate system. It is important to take into account the atmospheric chemical composition, the concentration in which they are and the medium in which they are transferred to have a clearer idea of the environmental reality in which we live. The important factors to take into account are the area of study, altitude and latitude, the climate it possesses and the surrounding environment, as well as the degree of urbanization, crop processes and industrialization.

To date, the characterization and quantification of atmospheric deposition has been carried out in specific environments, pursuing specific objectives. A study has been carried out in the city of Quito in 2010, but it is a research directed purely to a totally anthropized environment.

Due to all these arguments, this work is motivated by an urgent need to carry out a comprehensive study of the atmospheric contributions that occur simultaneously in different microenvironments of a geographical area.

The present work will allow quantification and chemical characterization of atmospheric deposition at 3 strategic points in the province of Imbabura with different natural environments, ecosystems, altitudes with diverse land uses, with intense and varied anthropogenic atmospheric emissions in certain areas.

4 OBJECTIVES

4.1 GENERAL OBJECTIVES

Perform an analysis of the concentration and composition of the particles that are deposited in natural environments and anthropized on Imbabura.

4.2 SPECIFIC OBJECTIVES

- To determine the chemical composition of the insoluble part of the rainwater samples from different sectors using the dispersive energy X-ray spectrometer.
- To obtain the chemical composition of the soluble part of the rainwater samples from different sectors using Ion Chromatography, Continuous Flow Analyzer and Inductively coupled plasma atomic emission spectrometry.
- To quantify the elements found in the soluble and insoluble part of the rainwater samples of each of the chosen sites.

- To investigate the possible emission sources of the most outstanding particles

4.3 HYPOTHESIS

There are different concentration values and emission sources of aerosols present in Ibarra, San Antonio and Yachay due to different human impact and altitude.

5 METHODOLOGY

5.1 SAMPLING LOCATIONS DESCRIPTION.

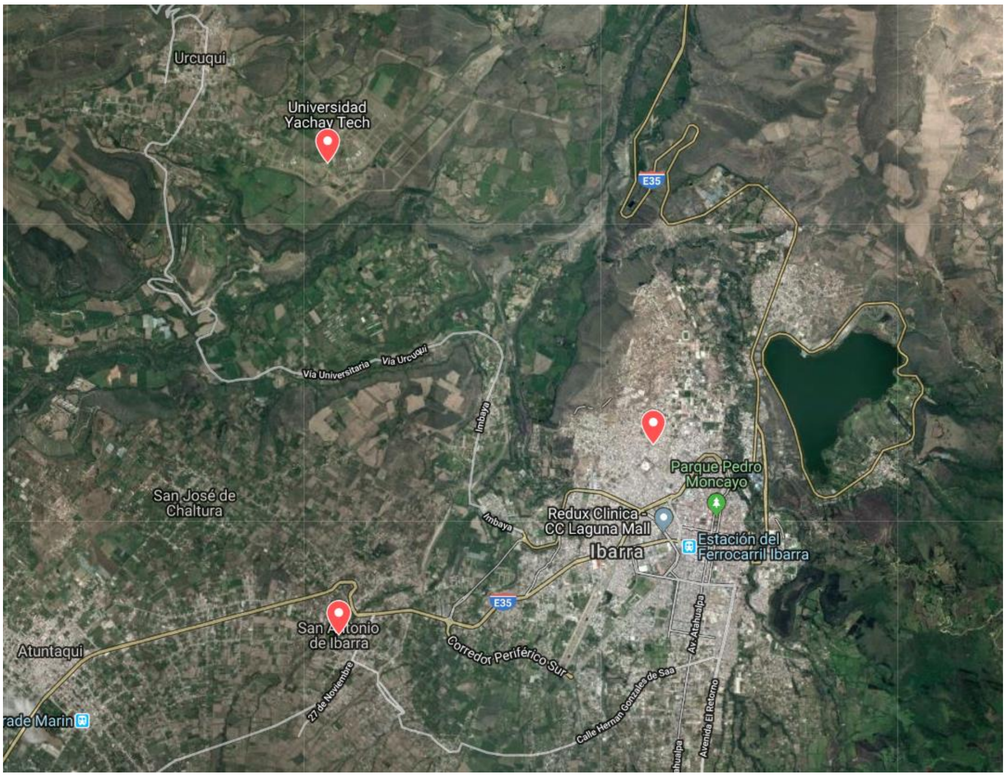

Figure 7. Location of rainwater collection samples. Reproduced from [39].

5.1.1 IBARRA

Ibarra is located in the province of Imbabura, borders with the province of Carchi, Pichincha, Antonio Ante and Urcuqui. Is located in the northern part of Ecuador It has an area of 1162.22km^2 which 41.68 km^2 correspond to the urban area and 1,120.53 km^2 to the rural area [58].

Climatology

The city of Ibarra has a mild dry climate, with an average annual temperature of 18 °C. The canton has an average temperature of 15.9 °C, in a range of 7 °C and reaches 25 °C [59]. Dates in 2013 show that rainfall varies between 5.8 and 78 mL. The months with the lowest rainfall correspond to the months from June to September [59].

In order to generate an idea of how precipitation values vary over a year in the city of Ibarra, the data collected from INHAMI in 2013 is shown in Table 5.

IBARRA-INHAMI (mL)											
November	December	January	February	March	April	May	June	July	August	September	October
35,7	22,5	8,8	77	41,2	31,3	78,5	4,5	13,3	12	5,8	42,2

Table 5. Precipitation values of INHAMI station in Ibarra city 2013. Reproduced from [15].

Description of sampling site located in Ibarra.

The sampling site is located in center of the city of Ibarra, an urban area surrounded by houses and buildings and completely exposed to vehicular traffic of the city. The geography location of the sampling site is 0.346387, -78.116627 and an altitude of 2215 mamsl.

Figure 8. Sample collection site in Ibarra.

5.1.2 SAN ANTONIO

San Antonio is located 5.50 km from the city of Ibarra, province of Imbabura. It has a territorial extension of 29.07km2. The height reached is between 2,040 mamsl and 4,620 mamsl [60].

Climatology

Compared to Ibarra, the parish of San Antonio de Ibarra has a cold climate at the top of the moorland of 2,800 to 4,620 mamsl and temperate climate towards the center of the parish at 2,040 meters at 2,800 meters; It has a rainfall of approximately 600 to 1000 mm, its average temperature is 9.8 ^{o}C in the upper part and reaches 17 ^{o}C in the lower part [60].

Description location of San Antonio de Ibarra

The sampling location is located in the sector Angarrumi considered an urban area with a geographical location of 0.2992410, -78.1844727 at an altitude of 2765 mamsl. Sector is influenced by the presence of vegetation and crop planting. By its geographical location it is possible to affirm that it is a little anthropized sector. In its surroundings that mostly crops and large green areas are found.

Figure 9. Sample collection site in San Antonio.

5.1.3 URCUQUI

San Miguel de Urcuquí, is located in the Province of Imbabura, It have a territorial area of 757 Km^2. Urcuquí limits to the east and north with the canton Ibarra, to the south and southwest with the cantons Antonio Ante and Cotacachi and to the west with the province of Esmeraldas. According to its topography, it is between 1,600 meters mamsl and 3,180 mamsl [61].

Climatology

Urcuqui canton has a temperate climate with an average temperature of between 16 ^{o}C at a height of 1400-3999 Urcuqui canton has a temperate climate with an average temperature of between 16 at a height of 1400-3999msnm and 19 in the center of Urcuqui at a height of 1600- 3180 masl. and 19 ^{o}C in the center of Urcuqui at a height of 1600- 3180 masl [61].

Description location of Urcuqui

The sampling collection is Yachay Tech University with a geographical location of 0.403827, -78.172612 and an altitude of 2058mamsl. The collection site is influenced by dust particles and building material generated at the site.

Figure 10. Sample collection site in Yachay.

5.2 SAMPLING METHOD

The rainwater samples collected were for one year beginning in the month of November 2018 and ending the month of November 2019. The collection was carried out on the first 4 days from the month of November 2018. The amount of Sample collected monthly is detailed in Table 6.

The sampling process begins with the collection of samples at the three sites mentioned above for one year. Each month, the integrated dry and wet deposition accumulated in the collectors was obtained. The collectors are a funnel adapted to a drum as shown in the Figure 11. When collecting the drum, distilled water was used to wash the funnel and collect the particles that were in the funnel. The surrounding, bottles of main bottle with funnel are just used to stabilize and prevent slippery. Once in the laboratory each of the samples were prefiltered with coffee filters to retain the residues that were accumulating in the collectors (leaves, arcs etc.). Once these were done, the filtration system observed in Figure 12 was used.

After the samples were filtered heave quartz fiber filters (45um) to separate insoluble material. The filtrate with soluble material were collected and stored at 5°C until transferred from Ecuador to Spain for analysis.

Figure 11. Model of Collector sample.

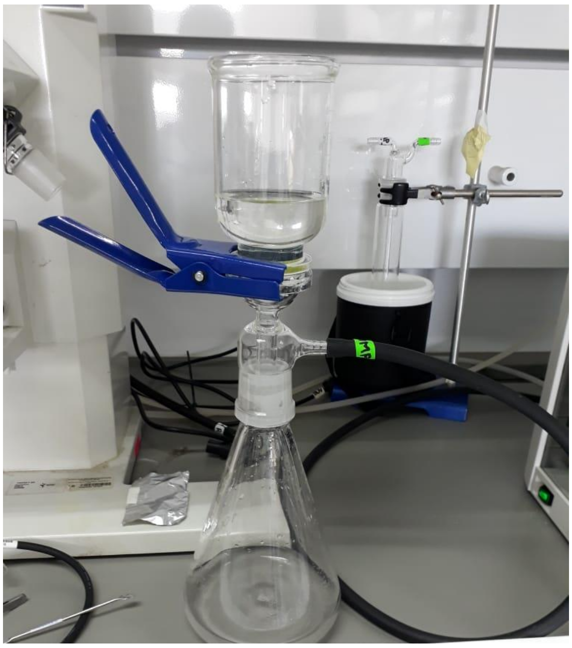

Figure 12. Water filtration system of samples

6 DESCRIPTION OF THE USED EQUIPMENT

6.1 X-RAY FLUORESCENCE BY DISPERSIVE ENERGY.

X-ray spectrometer of dispersive energy is an equipment whose main objective is to generate chemical composition data of elements present in samples. The technique he handles is not destructive and does not require prior sample preparation. Unlike an X-ray spectrometer the EDXRF incorporates measuring the energy of the characteristic radiation that comes directly from the sample. A dispersive energy X-ray spectrometer is composed of excitation source, fluorescence radiation detector and multichannel analyzer. The quality of the results will depend on the optimal work of these mentioned elements [62].

Initially the primary x-rays of the x-ray tube radiate the sample and excite the fluorescent radiation emitted by the sample and is recorded by the detector. The x-ray tubes use high voltages and currents of controllable currents in a range of 1 and 50 kV that guarantees the excitement of the elements found in the sample. It is possible to use two types of detectors such as semiconductors Si (Li) and HPGe. These detectors need to be exposed to liquid nitrogen cooling for use [63].

The concentration values of the elements are recorded in a spectrum by measuring the intensity of the energy associated with each electron transition. In other words the intensity of radiation as a function of energy [62].

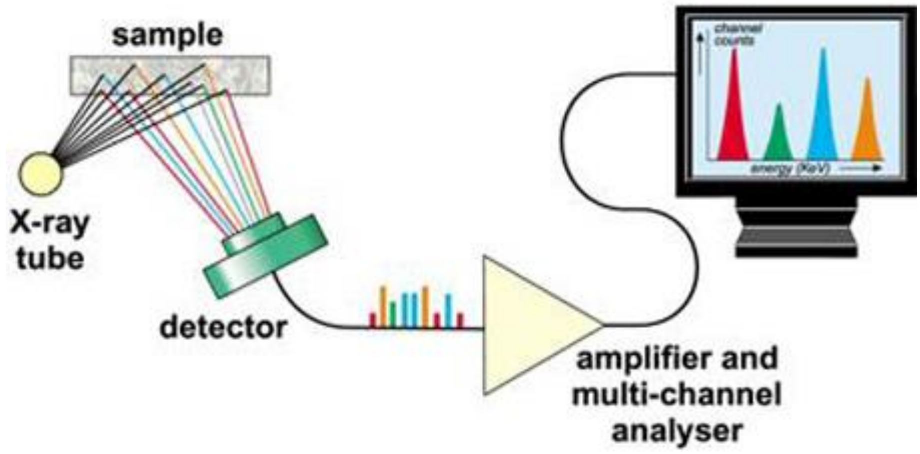

Figure 13. Scheme of measurement of EDXRF expectrometer. Reproduced from [64].

6.2 ION CHROMATOGRAPHY

Ionic chromatography is a high performance analytical technique for ion determination. To carry out the procedure, an eluent and the stationary phase are necessary. A pump is used for the continuous flow of the solvent in which it is mixed with the sample. The sample will travel through the column in which the ions present in the sample are separated depending on the affinity towards the column. Once this is done, they pass through a conductivity detector and depending on the retention time it is possible to compare each ions with a reference [65].

Figure 14. Ion Chromatography. Reproduced from [66].

6.3 CONTINUOUS FLOW ANALYZER

Continuous flow analysis (CFA), the sample is introduced into a solution that will flow through small tubes that detect the components of the sample. A color develops and the concentration of the sample is determined [67].

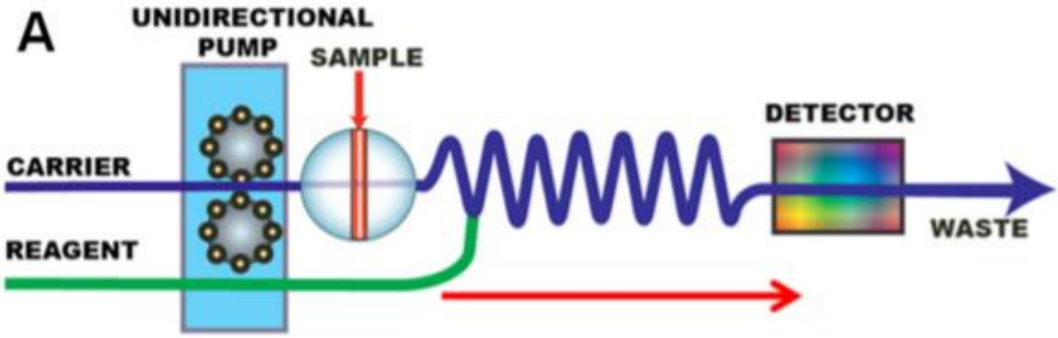

Figure 15. Scheme of measurement of Continuous Flow Analyzer. Reproduced from [68].

6.4 INDUCTIVELY COUPLED PLASMA ATOMIC EMISSION SPECTROMETRY

It is an analytical method that allows the quantitative determination of trace elements in aqueous samples. Initially, the aqueous sample is transported to the peristaltic pump to the nebulizer. In this part the sample is transformed into gas. This is transported to the ionization zone. In which a plasma is formed by the action of subjecting a flow of argon gas to an oscillating magnetic field induced by a high frequency current. By action of the ionization zone the atoms of the sample are excited and when they return to their fundamental state they emit characteristic wavelengths for each one. Finally, the detector will measure the intensity of the radiation by relating it to the concentration, this for each of the elements in the sample [69].

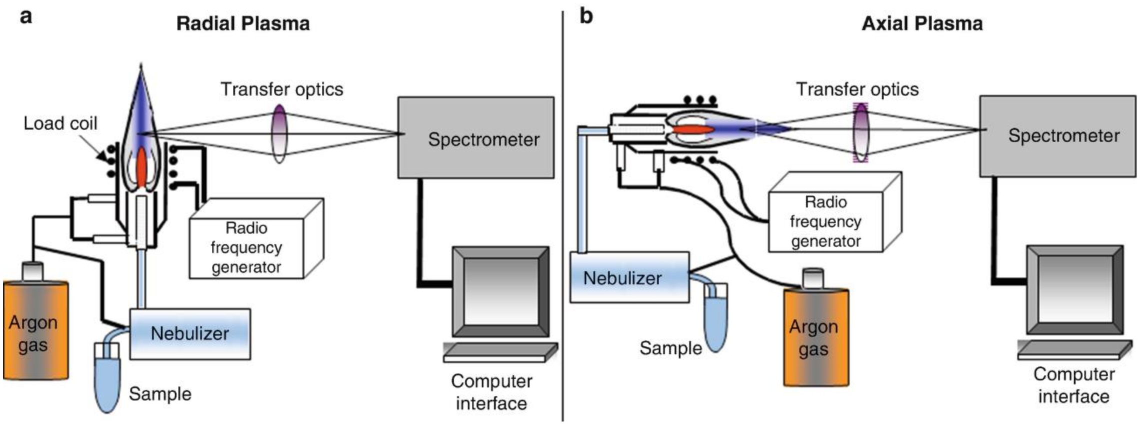

Figure 16 Scheme of Inductively coupled plasma atomic emission spectrometry. Reproduced from [70].

7 RESULT AND DISCUSSION

7.1 VOLUME OF THE COLLECTED SAMPLES

Table 6 shows the volume of samples in mL that was collected month by month from November 2018 to October 2019. Some samples could not be collected due to problems with the drums.

	Monthly Volume of the Samples (mL)											
Location	**November**	**December**	**January**	**February**	**March**	**April**	**May**	**June**	**July**	**August**	**September**	**October**
Ibarra	4010	144	2486	3685	3220	3750	3700	424	186	310	4995	4068
San Antonio	5610	166	1919			3274	5140	751	355	254		
Yachay	6110	640	4972	4306	1180	2570	2150	78	255	300	5540	5647

Table 6. Volume in mL of samples collected in Ibarra Yachay and San Antonio.

Figure 17 shows the graphical representation of the sample volumes from Table 6.

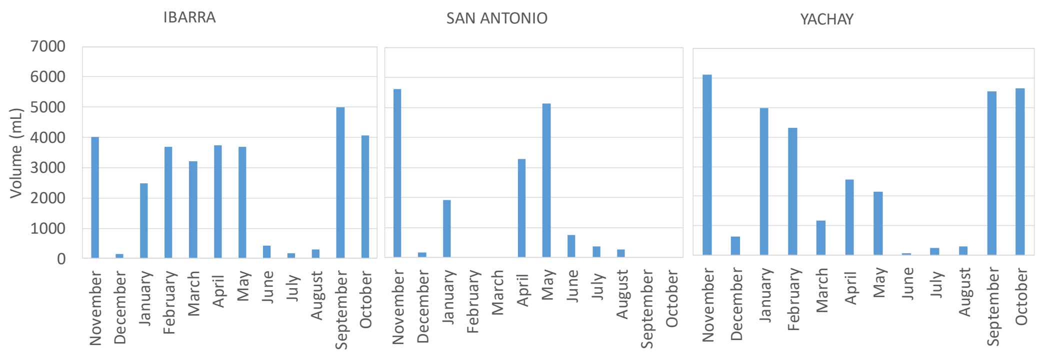

Figure 17. Graph of the volumes of the samples in Ibarra, San Antonio and Yachay.

Table 7 shows the amount of rainwater that the collector is able to collect in each month. This also depends on the amount of rainfall generated in each month.

Funnel Area		Amount of rainwater sample collected (L / m^2)											
0,047 m^2	Location	Novembe	December	January	February	March	April	May	June	July	August	Septembe	October
	Ibarra	81,687	2,933	50,642	75,066	65,594	76,390	75,372	8,637	3,789	62,131	101,752	82,868
	San Antonio	114,280	3,382	39,091	-	-	66,694	104,706	15,298	7,232	66,062	-	-
	Yachay	124,465	13,037	101,283	87,716	24,037	52,353	43,797	1,589	5,195	88,511	112,854	115,034

Table 7. Amount of rainwater sample collected (L/m2).

7.2 MATERIAL INSOLUBLE- FILTERS

The filters with insoluble material of samples collected only from November to June were analyzed due the logistic issues.

Figure 18. Filter results of the November, December and January.

The analysis of the resting samples (July – October) will be performed in near future. In the samples, the chemical concentration of Al, Si, Ca, Fe, P, K, Ti, Na, Mg, S, Cl, Sc, V, Cr, Mn, Ni, Cu, Zn, Ge, As, Se, Br, Rb, Sr, Y, Nb, Mo, Ag, Te, Ba, W, Pb, Bi were analyzed. All results are presented in Annex 1.

These results were separated in different graphs according to the concentration levels of each element for a better appreciation.

7.2.1 Al, Si, Ca and Fe.

Elements of Al, Si, Ca, and Fe of the insoluble samples were analyzed using the technique dispersive energy X-ray spectrometer give the following results.

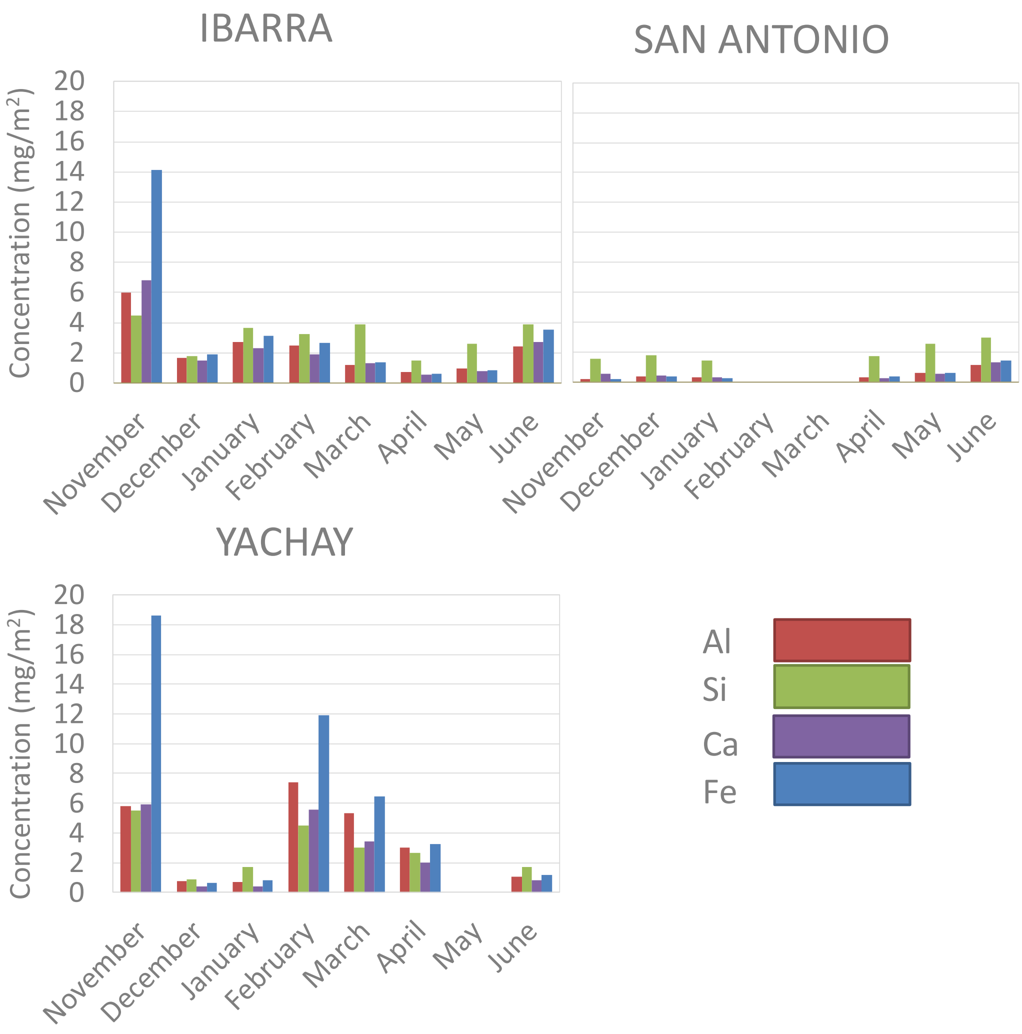

Figure 19. Concentration of Al, Si, Ca, and Fe retained over month from November to June and expressed as mg over m^2 of recollecting area in each sampling site.

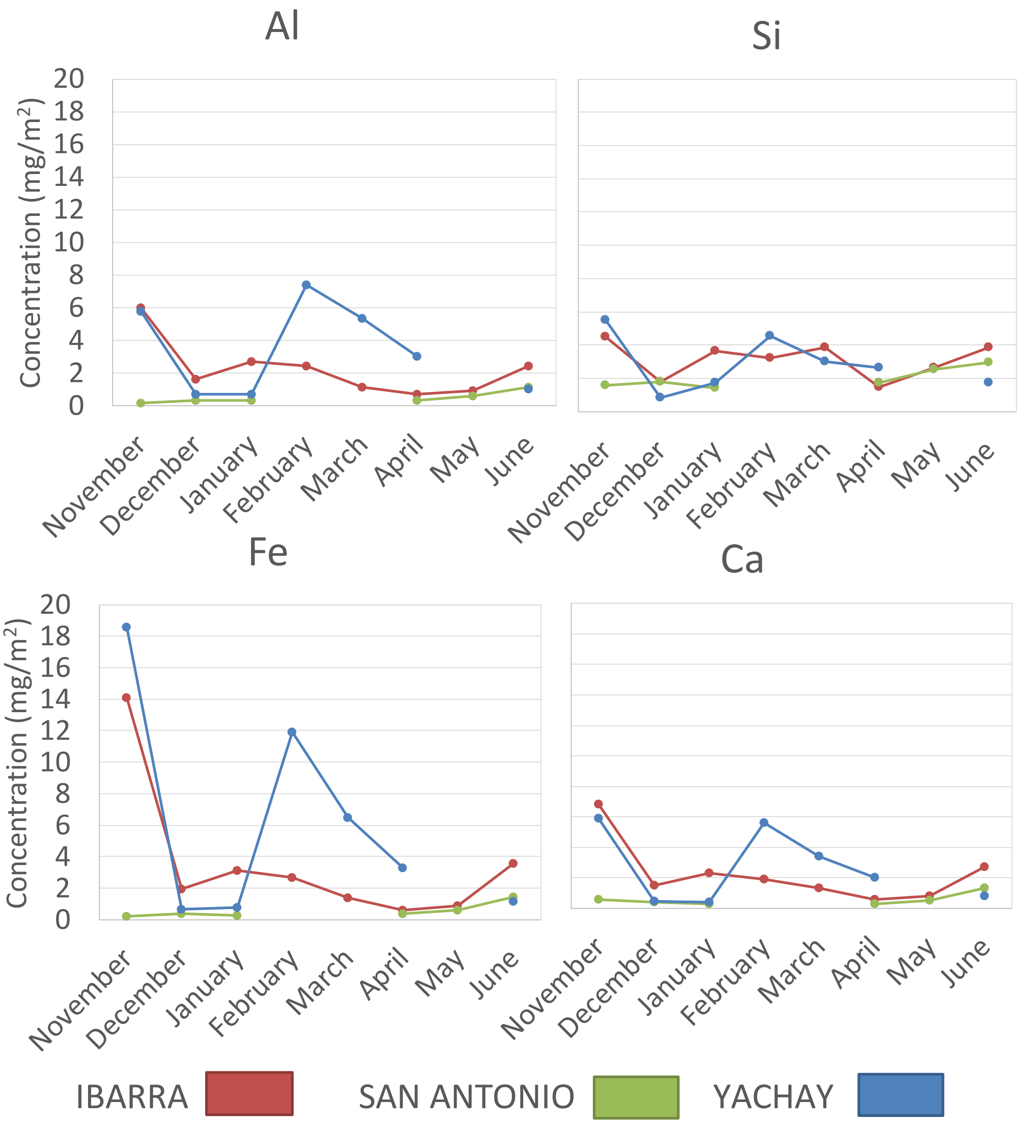

Figure 20. Concentration trends of selected elements expressed as a mg over m^2 of recollecting area.

Figure 19 shows the concentration values of Al, Si, Ca, and Fe. Concentration values vary between 0.18 - 18 mg/m^2. In Ibarra concentration values vary between 0.73 - 14.12 mg/m^2. San Antonio concentration values vary between 0.28 – 2.94 mg/m^2 and Yachay concentration values vary between 0.42 – 18.60 mg/m^2.

At first glance you can see that there is a greater concentration of these elements in Ibarra and Yachay. Al, Si and Fe reach higher concentration values in Yachay and Ca in Ibarra.

Aluminum, Silicon, Calcium, are typical elements of soil materials, construction and the earth's crust. This could explain the greater presence of these elements in Yachay because it is a site where street improvement works have been carried out. Iron is more related to fuel emissions from cars or road dust although it is also part of the cement raw material, although in a lower concentration. The presence of iron in the city of Ibarra could be explained because it is a more populated area and affected by vehicular traffic. Iron in the cement raw material would explain the presence in Yachay. Although vehicle emissions may also have influenced in the presence of iron in the zone by increase in vehicular traffic in Yachay because it is a developing area.

Figure 20 shows trend of each of the elements in the three sites. Aluminum, silicon, calcium, iron, cations have a very similar trend line in Ibarra, San Antonio and Yachay, This could be associated with the fact that the elements come from the same source of origin.

At first glance it can be seen that the concentrations in the month of November are higher compared to December. This could be explained because in this first month the pre-filtering process with the coffee filters was not carried out. Another aspect that stands out in the graph is that there is a high concentration of the elements in the month of February in Yachay. It could be due to some gust of wind came out near the sampling site. Regardless of the peaks that stand out in the month of November and February, the elements are in a range of 0.18 - 4 mg/m^2.

7.2.2 P, K, Na, Mg

Elements of P, K, Na and Mg of the insoluble samples were analyzed using the technique dispersive energy X-ray spectrometer give the following results.

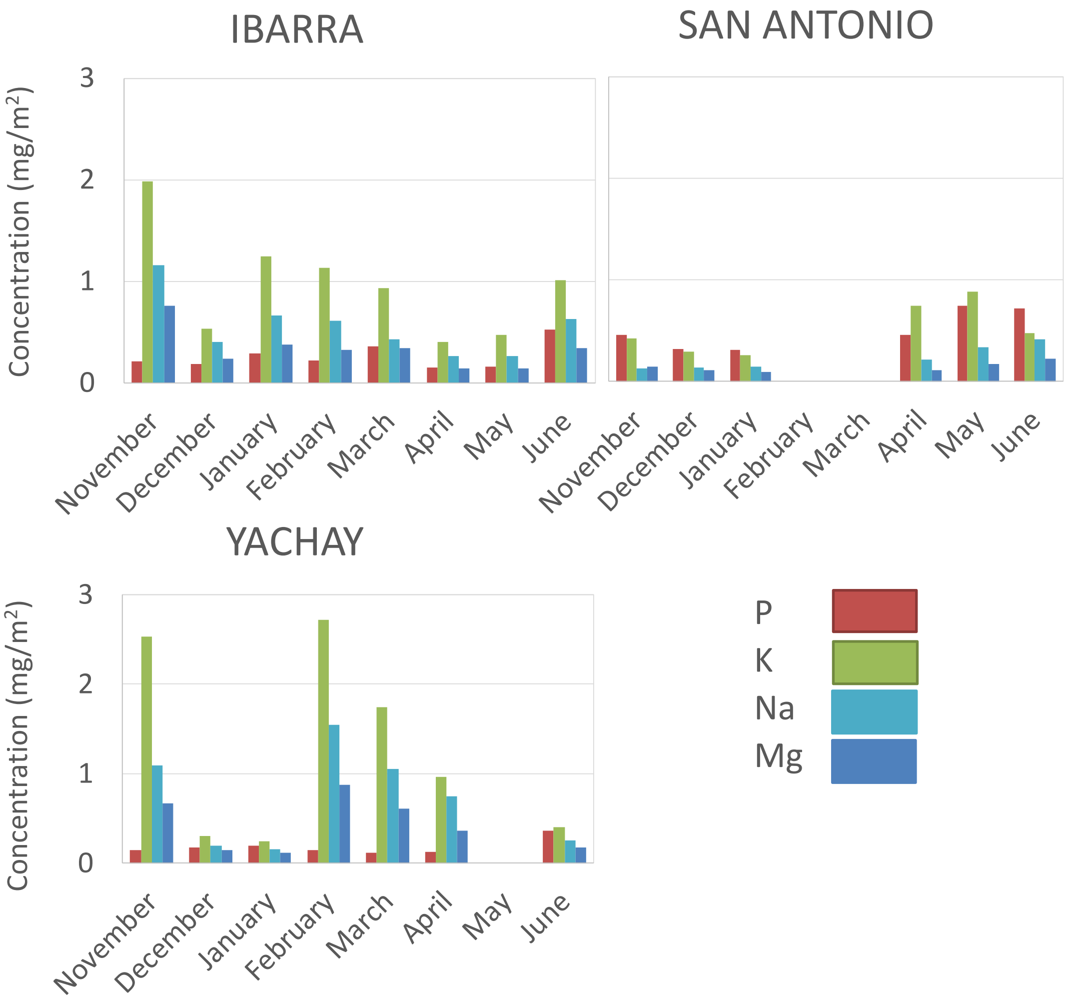

Figure 21. Concentration of P, K ,Na and Mg retained over month from November to June and expressed as mg over m^2 of recollecting area in each sampling site.

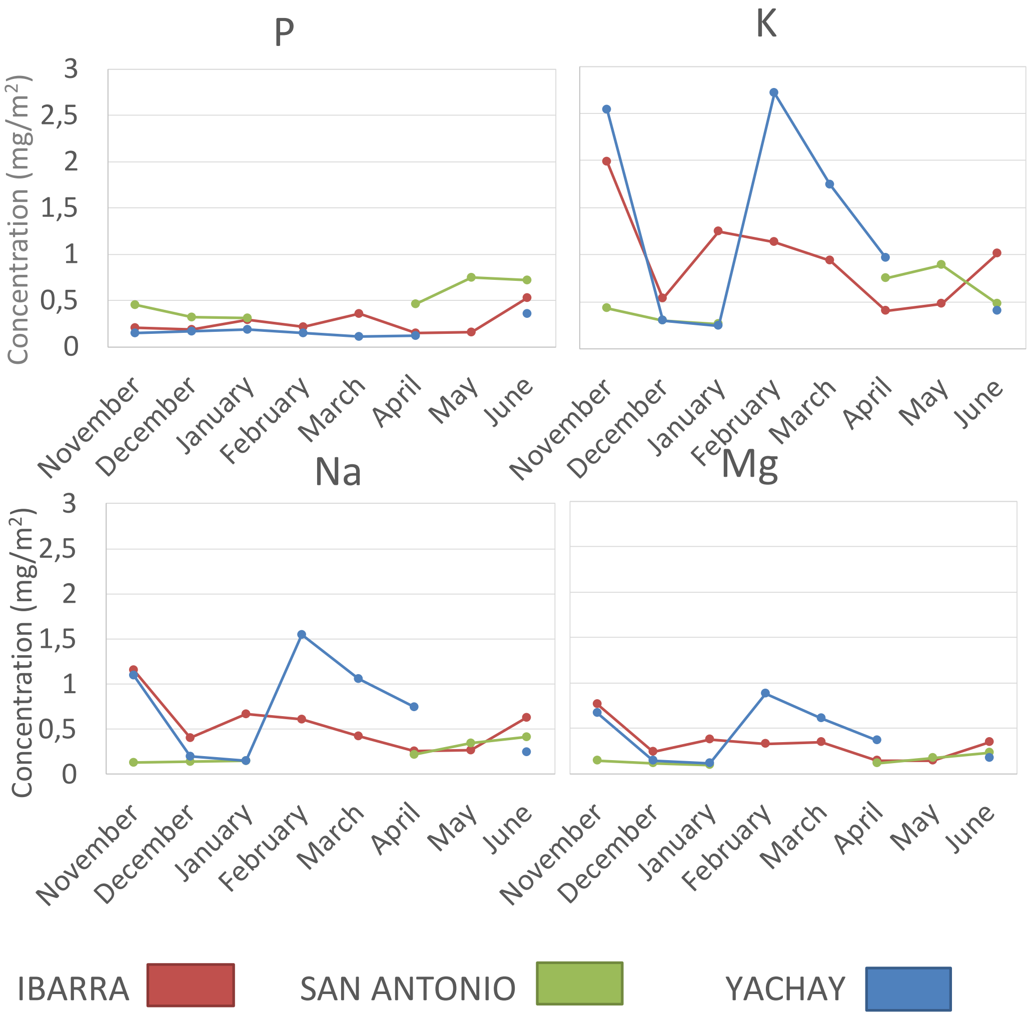

Figure 22. Concentration trends of selected elements expressed as a mg over m² of recollecting area.

Figure 21 shows the concentration values of P, K, Na and Mg. The concentration values vary between 0.0563 – 10.168 mg/cm^2. In Ibarra concentration values vary between 0.09 – 1.98 mg/m^2. San Antonio concentration values vary between 0.03 – 0.88 mg/m^2 and Yachay concentration values vary between 0.06 – 2.72 mg/m^2.

In general terms it can be seen that the elements have higher concentrations in Ibarra and Yachay.

Potassium is a common element in the raw material of cements, soils and is even used in the chemical composition of fertilizers. These emission sources can explain their presence at the three sampling sites.

Potassium in Yachay is associated construction process, works in the streets that have generated wind gusts in the place. Ibarra that presents a significant value of this potassium could be due to some of sources similar to those of Yachay. The presence of potassium in San Antonio may be due to the organic material of the plants that accumulated in the drums.

Marine aerosols from the seas are mainly a source of Na but also of Mg as MgCl, MgSO4 are present. Figure 23 shows wind paths from the Pacific Ocean to Imbabura in the February month. HYSPLIT database presents the paths with red blue and green lines. This could justify the presence of these elements in the three sampling sites.

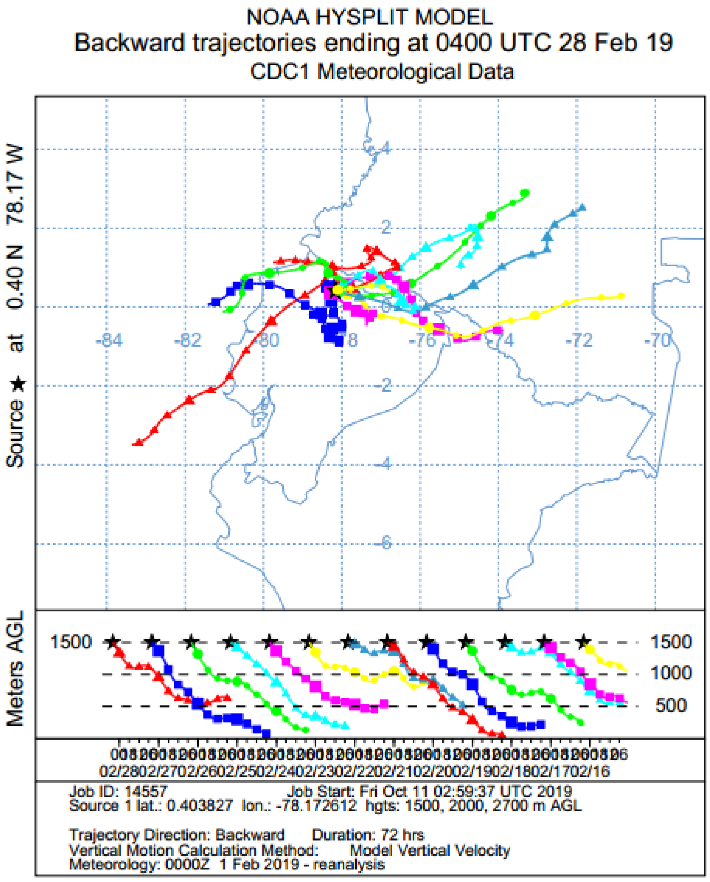

Figure 23. Wind path that reached Imbabura in the month of February using HYSPLIT

Although magnesium, being part of the chemical composition of fertilizers that generates the green color to the plants, would also explain the presence of this element in San Antonio since, as previously stated in the collectors, organic material accumulated.

Phosphorus comes mainly from organic wastes, fertilizers and wastewater. This is consistent with the presence of a high concentration of phosphorus in San Antonio because it is a more natural sector in which agricultural and livestock production uses and generates this source.

Figure 22 shows the trend of each of the elements in the three sites. In this graph you can also see that the concentrations in the month of November are higher compared to December. As stated earlier it is due to that the prefiltering process with the coffee filters were not carried out. In the same way, Na, K, Mg have a high concentration in February in Yachay. As already mentioned above it can be the product of gusts of wind that could increase the concentration of these elements.

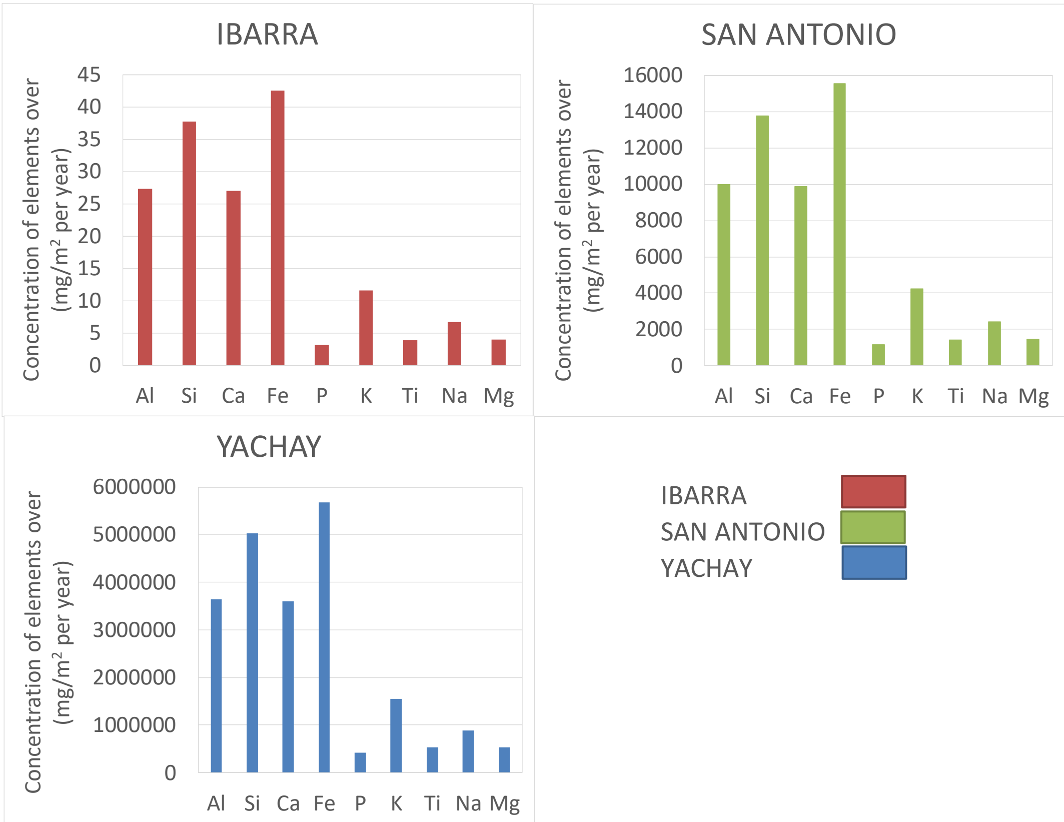

Figure 24. Element flux deposition of select elements in three different sampling site normalized over year and expressed as mg element deposited over m^2 of recollecting area.

Figure 24 shows higher concentration peaks of Al, Si, Ca and Fe. It is probably that sources of emission of these elements are the most abundant in the part of Imbabura.

7.3 MATERIAL SOLUBLE – RAINWATER

7.3.1 pH

One of the data that was also determined was the pH. The results are shown below.

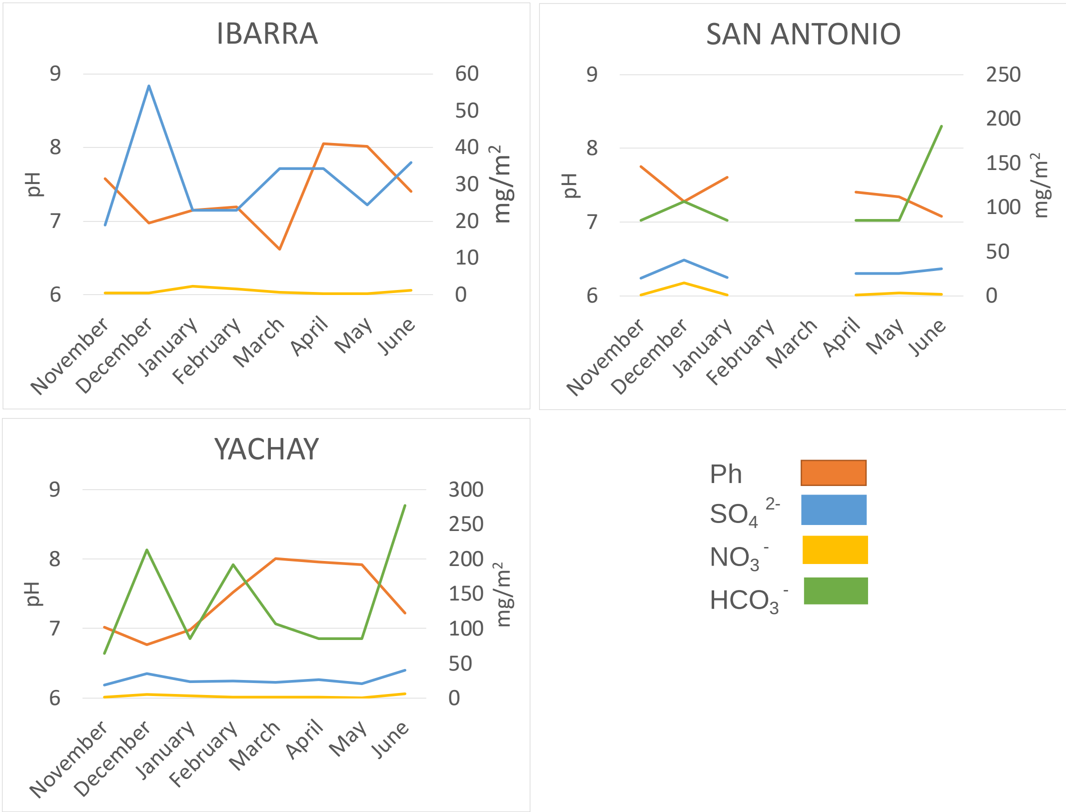

Figure 25. Graph of pH values in Ibarra, San Antonio and Yachay and comparison with SO_4^{2-}, NO_3^- and HCO_3^-.

Figure 25 show the pH values of rainwater in each month of the different sampling sites. The values range from 6 to 8. This would show that there is no acid rain present in any of the 3 sampling sites; rather all the results would show that the samples are alkaline. In each of the graphs the pH was related to the emissions of HCO_3^-, SO_4^{2-} and NO_3^-. In each month of sampling, it is observed that while the concentration of emissions increases, the pH decreases. This is because there are high concentrations of these emissions; sulfuric acid, nitric acid and carbonic acid are formed in the air, which are the main compounds that increase the acidity in rainwater.

7.3.2 CONDUCTIVITY

The conductivity values of the soluble samples were determined. The results are shown below.

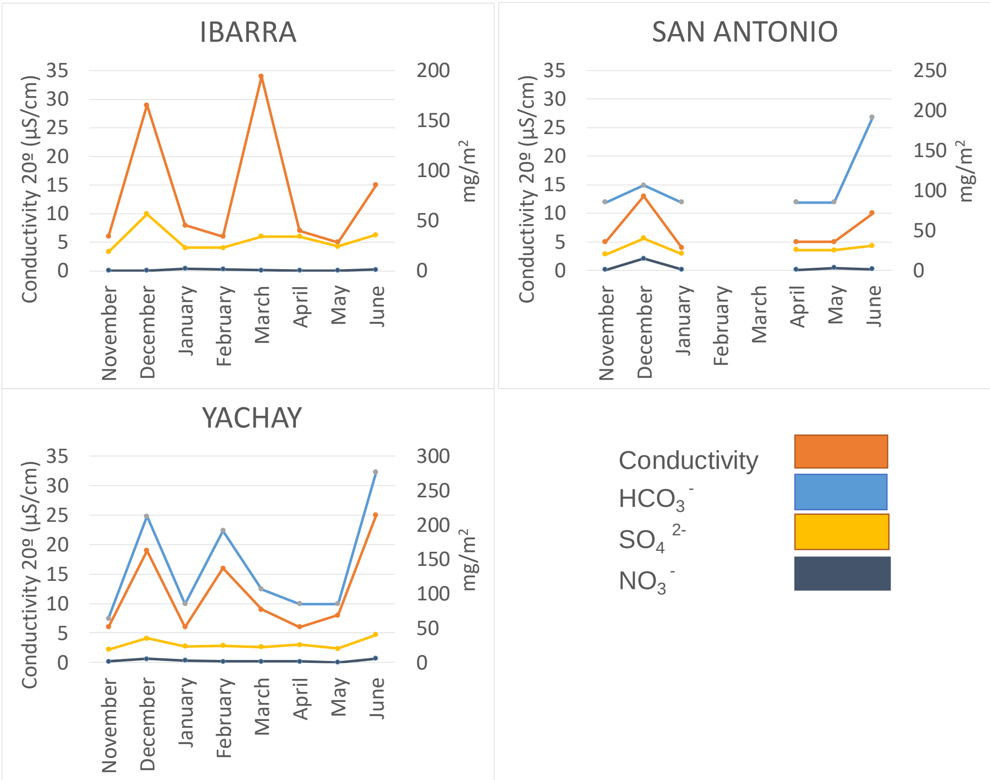

Figure 26. Graph of conductivity values in Ibarra, San Antonio and Yachay and comparation with SO_4^{2-}, NO_3^- and HCO_3^-

Figure 26 show the conductivity values of rainwater in each month and the different sampling sites. Values range between (4- 34) (µS / cm). In Ibarra, higher conductivity values achieve a range of (7-34) (µS / cm) compared with Yachay and San Antonio. The graph would show the relationship between the conductivity of rainwater and the concentrations of HCO_3^-, SO_4^{2-} and NO_3^-. As already mentioned in the theoretical section, the conductivity is related to the amount of ions dissolved in the water, the graph shows that the concentration of nitrate, carbonate and sulfate ions are directly proportional to the conductivity values of the collected samples.

7.3.3 TRACE METALS (Al, Ba, Cu, Cd, Fe, and V)

Trace metals Al, Ba, Cu, Cd, Fe, and V of the soluble samples were analyzed using the technique inductively coupled plasma atomic emission spectrometry give the following results.

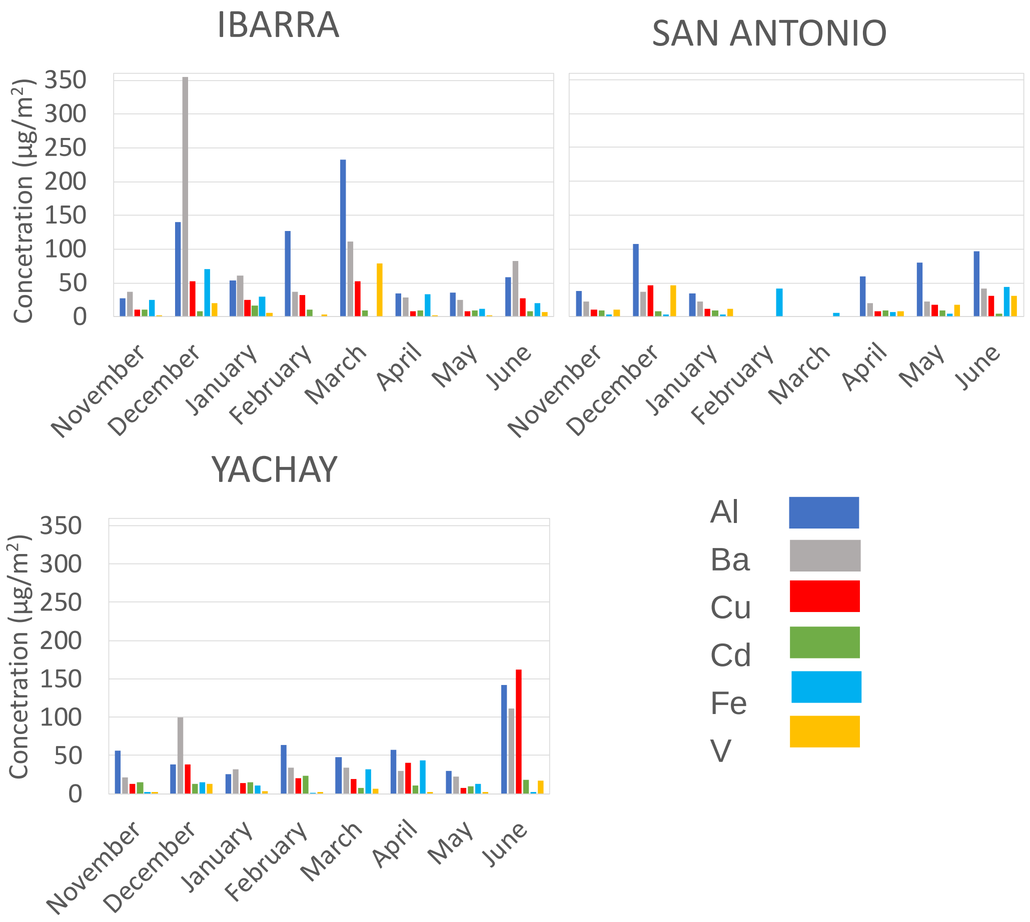

Figure 27. Concentration of Al, Ba, Cu, Cd, Fe and V retained over month from November to June and expressed as µg over m^2 of recollecting area in each sampling site.

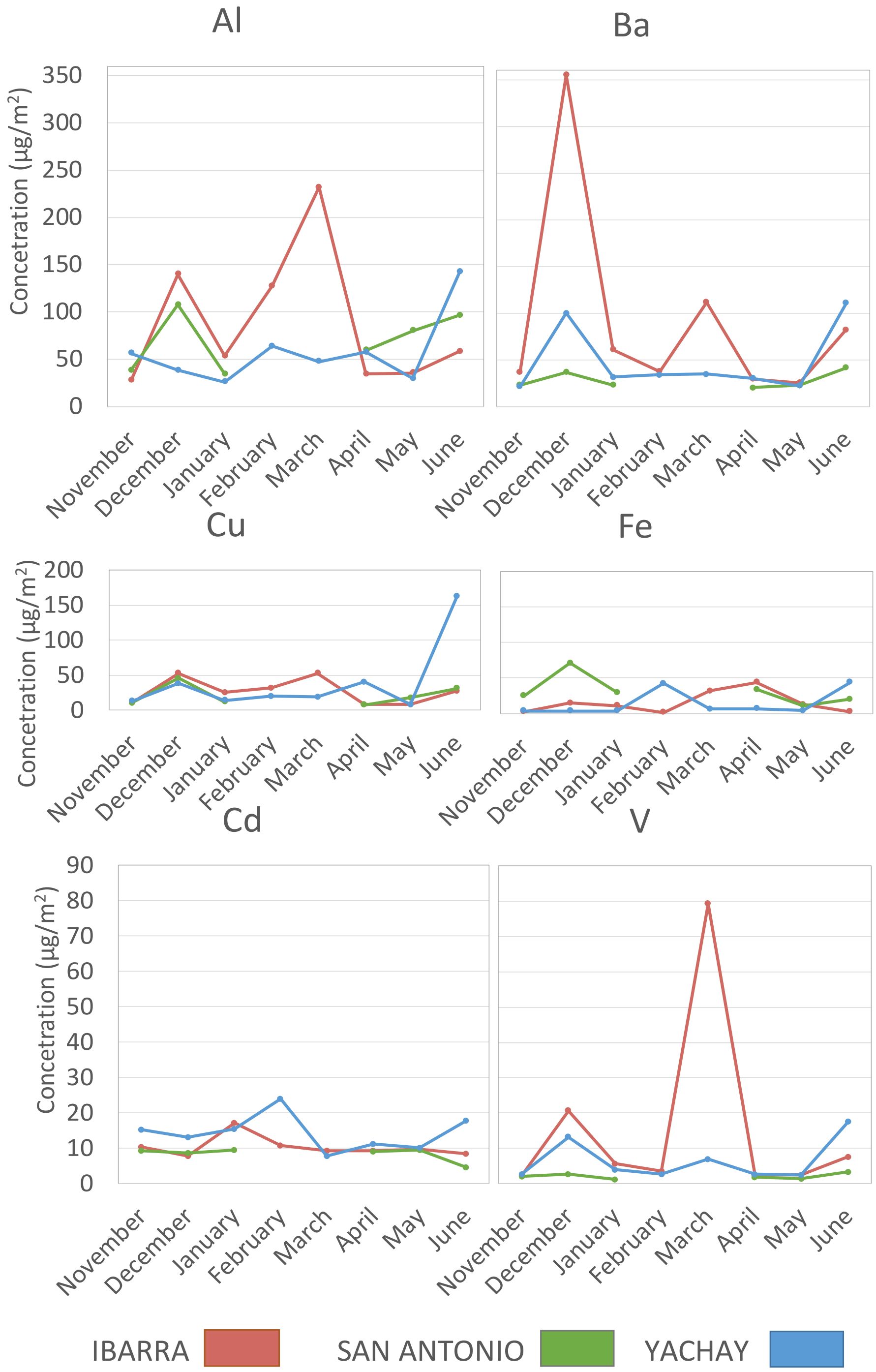

Figure 28. Concentration trends of selected elements expressed as a mg over m² of recollecting area.

Figure 27 shows the concentration values of Al, Ba, Cu, Cd, Fe and V. The concentration of Al varies from 34.26 – 231.91 µg / m², Ba between 22.34 – 351.31 µg / m², Cu 7.66 – 162.55 µg / m², Cd between 4.46 – 23.82 µg / m², Fe between 2.34 – 70.64 µg / m² and V between 1.04 – 13.19 µg / m² in Ibarra, San Antonio and Yachay from November to June.

Ba has a higher concentration value in Ibarra and Yachay compared to San Antonio. Ba achieves concentrations of 355.31 µg / m^2 and 110.85 µg / m^2 respectively. Al presents a high concentration in Ibarra in the months of December to March. Cu achieves highest concentration in Yachay in the month of June, a value of 162.55 µg / m^2. The concentrations of Cd, Fe and V not show a great variation in their concentrations. These elements range from 1.06 – 23.82 µg / m^2.

As already mentioned above, Al is typical mineral element, materials of soil, construction and the earth's crust. This may be associated with the use of sand, gravel and cement used by the different block manufacturing centers in the city of Ibarra.

The presence of Ba is associated with the production of paints, bricks, glass and rubber ceramics. This is consistent with the greater presence of this cation in Ibarra than in other locations. Ba is an element present in fireworks, which is a common practice in Ibarra at Christmas and New Year’s Eve. One of the sources of Cu emission is cement production; this could be related to the construction processes that Yachay has carried out.

The presence of Fe is also seen in the results of rainwater samples, the sources of this metal are mainly industrial processes, fossil fuels and diesel emissions, in the same way as road dust and is also part of cement raw material, although in lower concentrations. The presence of Cd and V by fossil fuel combustion processes.

Figure 28 shows the trend of each element has had throughout November to June. What stand out in the graph are the high peaks that V, Ba and Cu show in March, December and June respectively. This could have been generated by some accumulation of these elements by factors such as precipitation frequency wind direction among others.

7.3.4 TRACE METALS (Zn)

Trace metals Al, Ba, Cu, Cd, Fe, and V of the soluble samples were analyzed using the technique inductively coupled plasma atomic emission spectrometry give the following results.

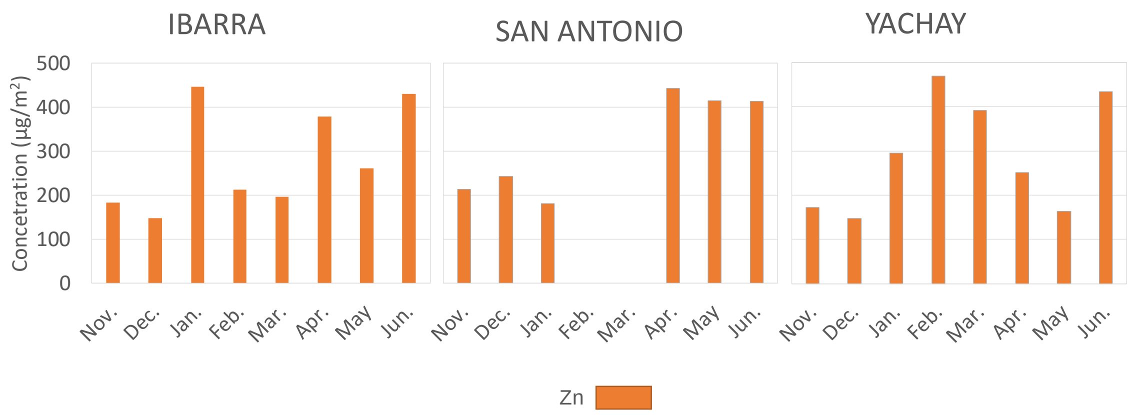

Figure 29. Concentration of Zn retained over month from November to June and expressed as µg over m² of recollecting area in each sampling site.

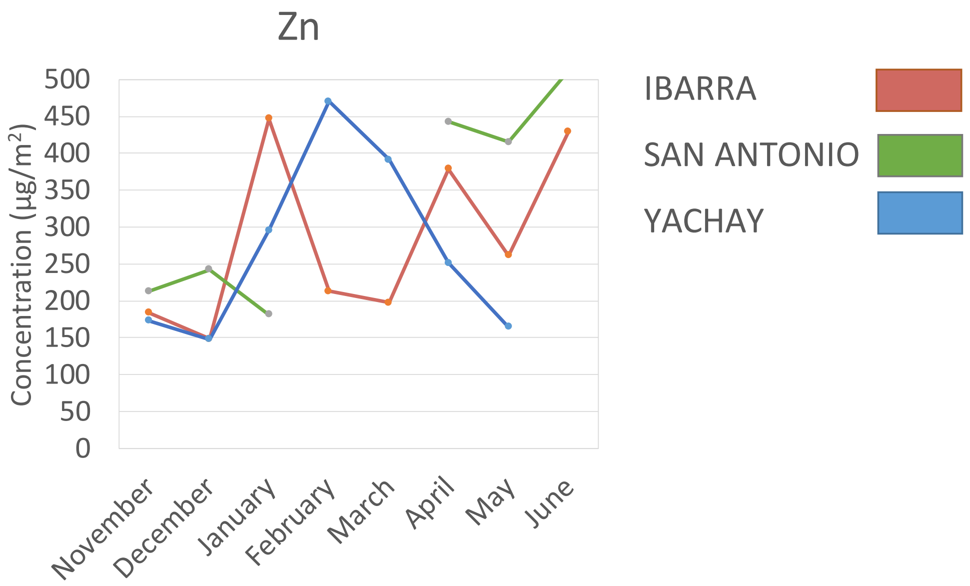

Figure 30. Concentration Trends of selected elements expressed as a µg over m2 of recollecting area.

Figure 29 shows that Zn concentration values vary at each of the sampling sites.

Ibarra has a concentration in a range of (148.29 - 446.80) µg/m^2. Yachay has a concentration of (147.87 – 470.21) µg/m^2. Compared to Figure 27, that the units are also in µg/m^2, it would be understood that in Zn it has greater concentrations than Al, Ba, Cu, Cd, Fe, V.

Previously it was mentioned that Zn can be released due to cement production processes since it is one of the main elementary contents of the raw material. But one of the causes that could have caused the Zn concentrations to be so high in each of the months is the mining exploitation that occurred in the parish of Buenos Aires, 15 km from the center of

Urcuqui. This mining exploitation has been taking place since the first months of 2018. and was controlled in July 2019.

Figure 30 shows a clear trend in each of the sites. In the months of January and February a displaced relationship is seen. This could be the cause of factors such as wind.

7.3.5 IONS ($Mg^{2+,}$ K^+,Cl^-, Na^+)

Ions $Mg^{2+,}$ K^+, Na^+ were analyzed using Continuous Flow Analyzer while Cl^- was analyzed with Ion Chromatography. These ions give the following results.

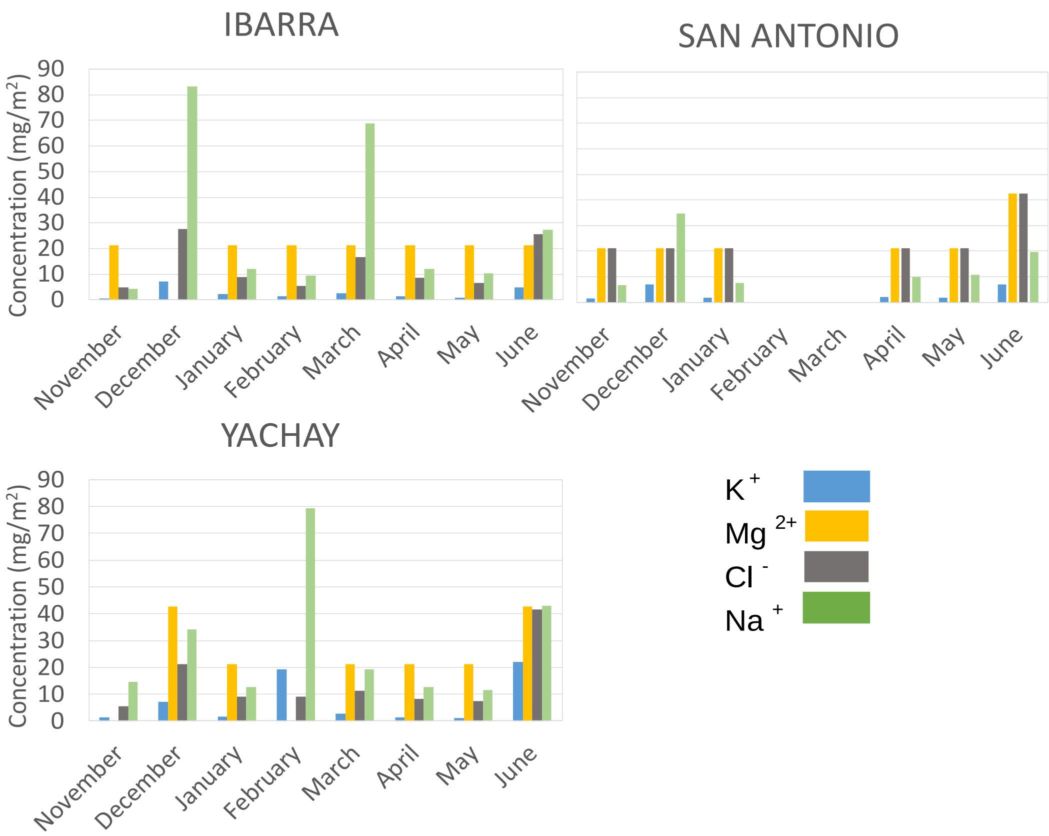

Figure 31. Concentration of K^+, Mg^{2+}, Cl^- and Na^+ retained over month from November to June and expressed as mg over m^2 of recollecting area in each sampling site.

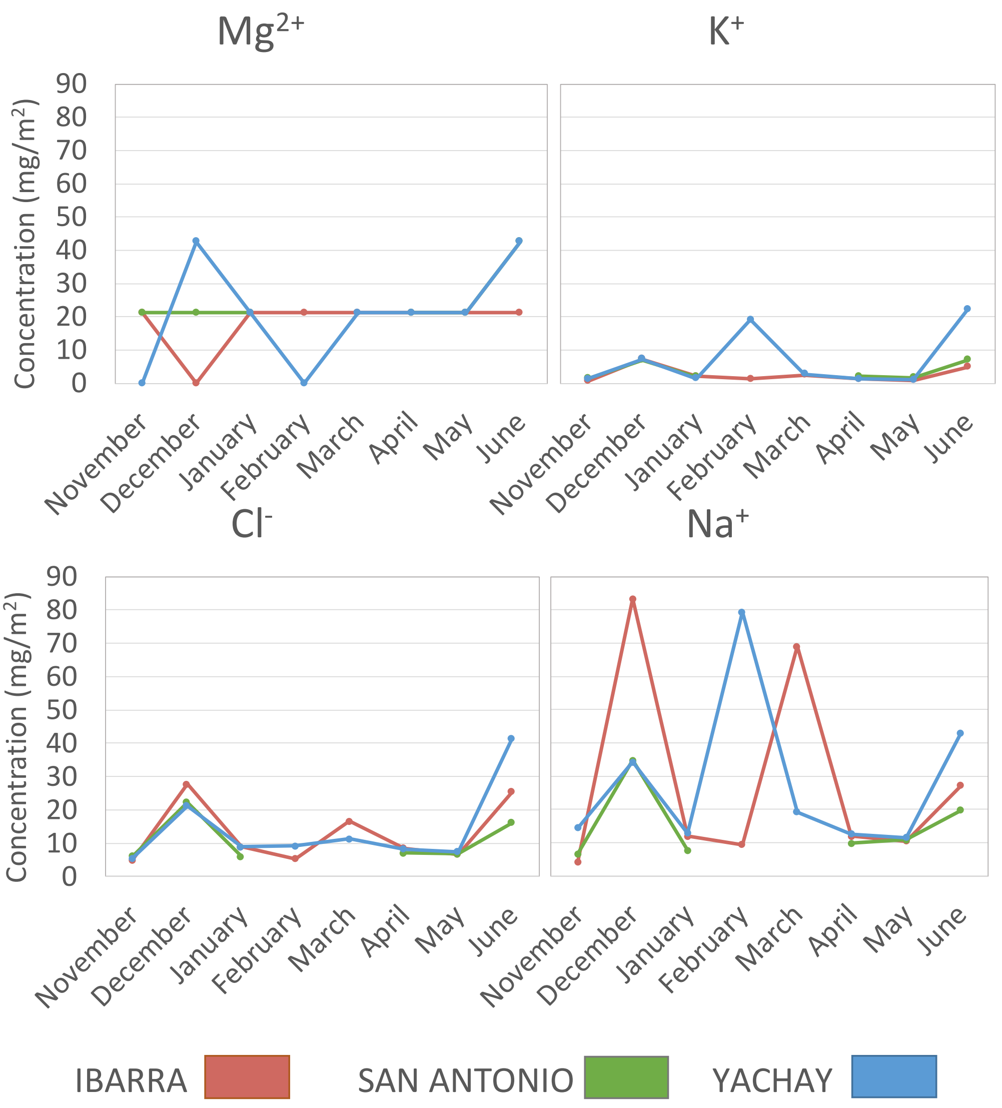

Figure 32. Concentration trends of selected elements expressed as a mg over m2 of recollecting area.

The composition values of K^+, $Mg^{2+,}$ Cl^- and Na^+ are shown in the Figure 31. In the Ibarra graph it can be seen that the concentration values vary between (0.85 - 3.92) mg /m^2. The results show changes in their concentrations throughout each month. From the graph it is important to rescue the high Na^+ concentration values in the months of December and March.

In the Yachay chart, the values vary from (0.85 - 79.36) mg /m^2 of this graph. It is important to rescue the high concentrations of Na^+ in the month of February.

In the San Antonio chart, the values vary from (1.48 – 34.68) mg /m^2 of this graph. It is important the high concentrations of Mg^{2+} and Cl^- in the month of June. Also is possible to appreciate a high concentration peak of Na^+ in the December month.

Figure 32 shows the tendency of each of the ions in each of the sites, although there is variation in its concentrations, K^+, Cl^-, Na^+ follow a trend while Mg^{2+} does not show that it follows a clear trend.

The significant presence of Mg^{2+} may be due to the importance of these elements in agriculture.

Marine aerosols are primarily responsible for the emission of Cl^- and Na^+ because they are the main elements present in ocean water. It is also important to consider wind speed and direction and the transport of air masses.

Figure 33, Figure 34 shows the influence of the air masses and the wind routes that come from the ocean in the February and march months that would be in accordance with the results that were previously shown in the Figure 31 in which there is a greater presence of Cl^- and Na^+ in the three different sites.

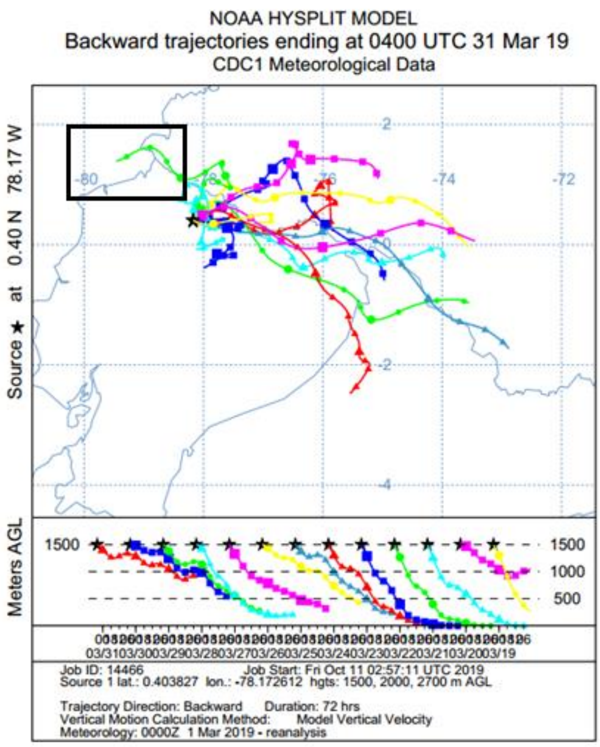

Figure 33. Wind path that reached Imbabura in the month of March using HYSPLIT [71].

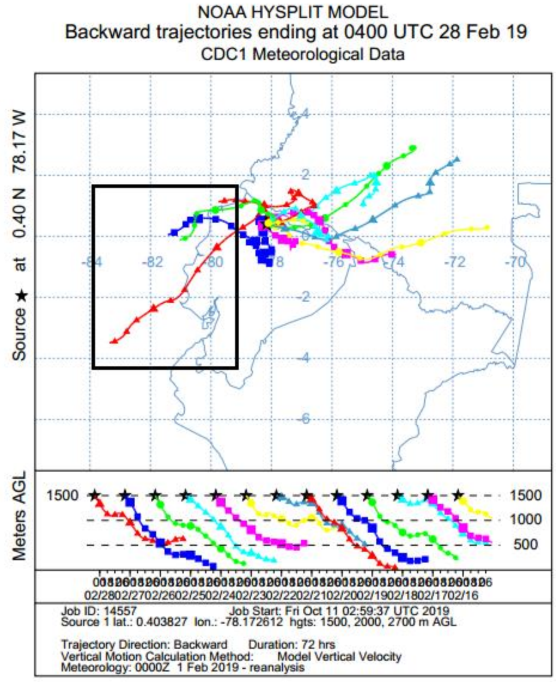

Figure 34. Wind path that reached Imbabura in the month of February using HYSPLIT [71].

7.3.6 HCO_3^-, SO_4^{2-}

Ions of HCO_3^- and SO_4^{2-} the soluble samples were analyzed using the technique Ion Chromatography give the following results.

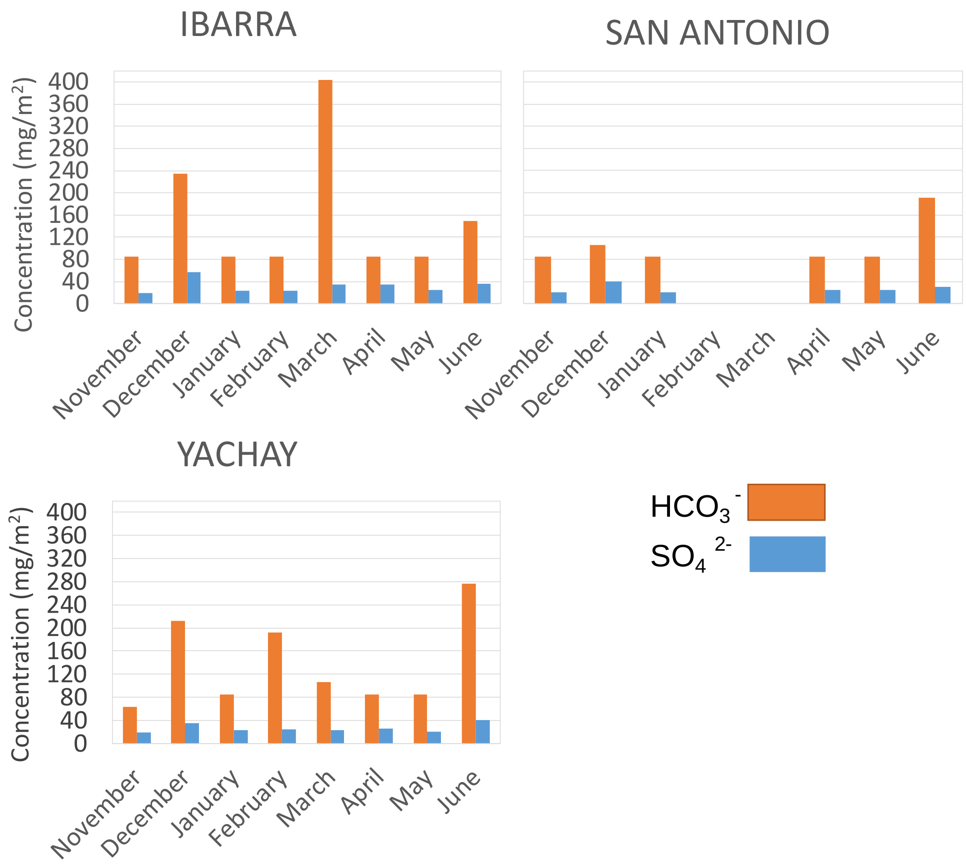

Figure 35. Concentration of HCO_3^- and SO_4^{2-} retained over month from November to June and expressed as mg over m^2 of recollecting area in each sampling site.

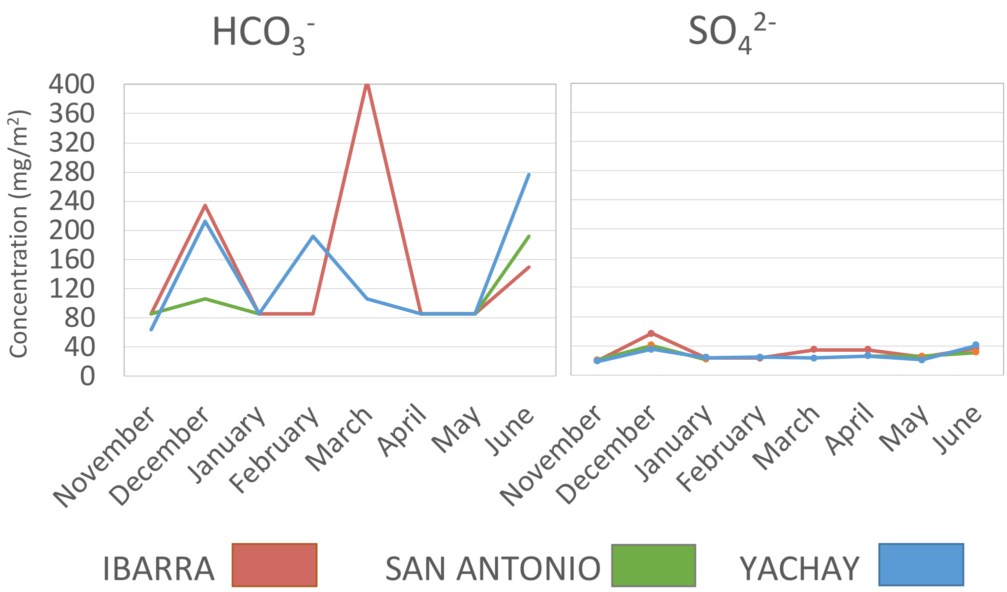

Figure 36. Concentration trends of selected elements expressed as a mg over m2 of recolleting area.

Figure 35 shows that the concentration values of HCO_3^- and SO_4^{2-} that vary between (20.85 – 404.25) mg/m^2. In each of the sites a high concentration of HCO_3^- is observed in comparison with SO_4^{2-}. In Ibarra it reaches a high concentration of 404.25 mg/m^2 in the month of March. In San Antonio it has a concentration of 191.48 mg/m^2 in the month of June and Yachay reaches a concentration of 276.59 mg/m^2 in the month of June.

Figure 36 show the tendency of HCO_3^- and SO_4^{2-}. Sulfate shows a very clear trend in which we could say that the emissions come from the same source while the bicarbonate does not show a clear trend.

In the case of SO_4^{2-} it is mainly due to volcanic emissions, production of cement or related materials and vehicular traffic. The graph shows greater concentration in Ibarra as it is a site influenced by the population and industrial processes. In comparison with the three sites, the city of Ibarra is more affected by sulfate.

The presence of HCO_3^- may be a consequence of CO_2 in the atmosphere by natural and anthropogenic emission sources. No environment will be free of CO_2. This pollutant when reacting with water forms carbonic acid and this will dissociate into hydrogen ions and bicarbonate ions.

$$CO_{2(g)} \rightleftharpoons CO_{2(ac)}$$

$$CO_{2(ac)} + H_2O_{(liq)} \rightleftharpoons H_2CO_{3(ac)}$$

$$H_2CO_{3(ac)} \rightleftharpoons H^+_{(ac)} + HCO_3^-$$

The Figure 35 shows a greater presence of the bicarbonate ion in Ibarra and Yachay, because they are more affected by pollution sources than San Antonio, which we consider to be a less anthropogenic sector.

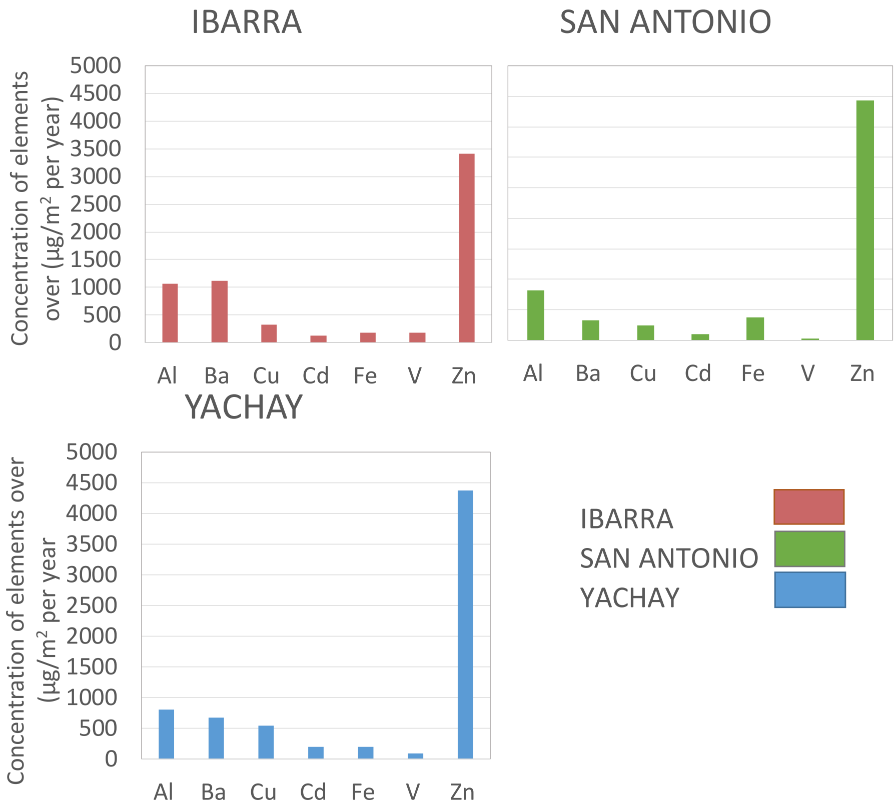

Figure 37. Element flux deposition of select elements in three different sampling sites normalized over year and expressed as µg element deposited over m² of recollecting area.

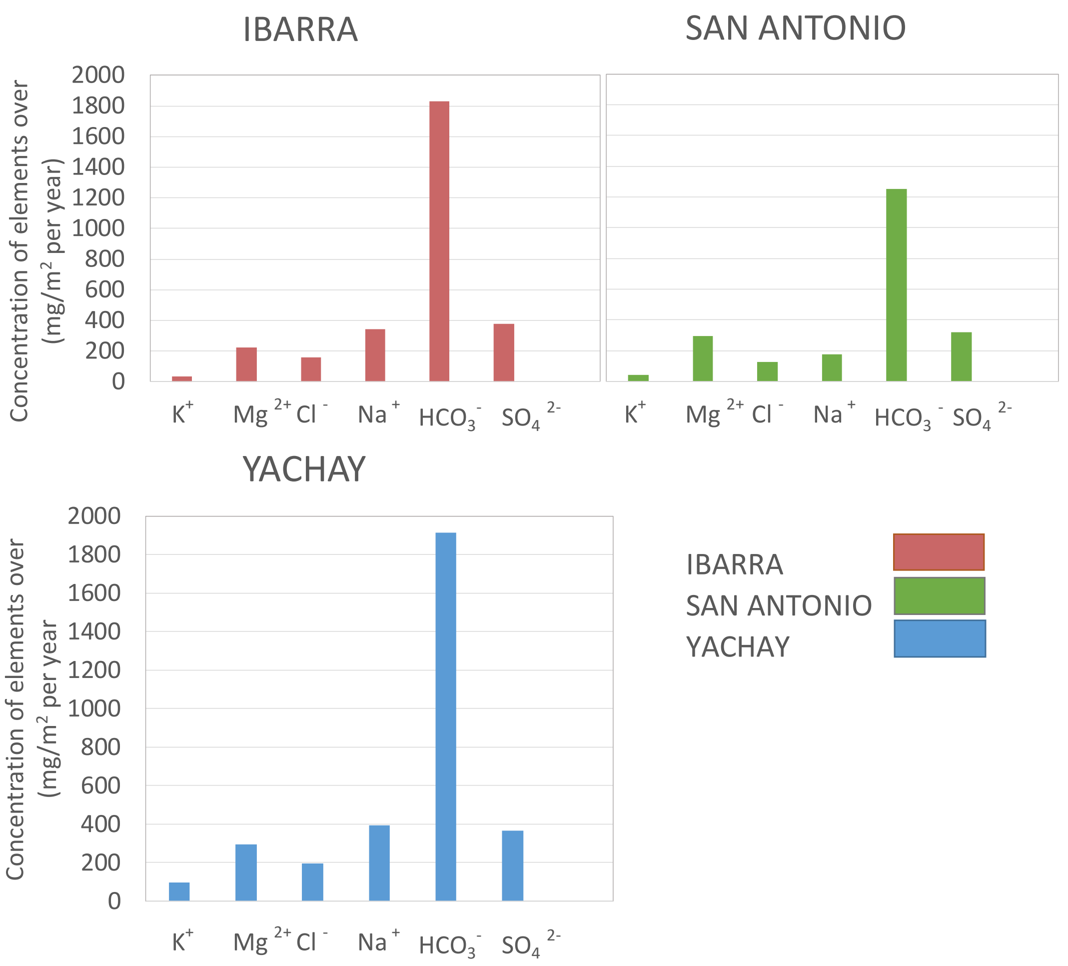

Figure 38.Ions flux deposition of select ions in three different sampling site normalized over year and expressed as mg element deposited over m² of recollecting area.

Figure 37 and Figure 38 It shows the quantity of each trace element and ions present throughout the collection time. In the graph of the elementary trace it is possible to see a high accumulation of Zn that predominates in the three sites. The presence of Zn is 4 times more than the concentration of the other elements.

The ion graph shows an accumulation of HCO3- in all three sites. The presence of bicarbonate is 8 times more than that of the other ions.

7.4 HEAVY METALS

In the tests performed there are presence of heavy metals such as Co, Hg, Mo Ti, V, Cr, Mn, Ag, Cr, Sb. In general, emissions are mainly anthropogenic sources such as gasoline combustion and industrial activity.

The results showed that the concentrations of these metals were minimal. But it would be important to keep them in mind for future analysis, especially in the study of the toxicology of these heavy metals.

8 COMPARATION WITH BOGOTA

In order to determine the state of pollution that we have in Ibarra, we have seen the need to determine a comparison with the city of Bogota. Much more populated than Ibarra but with geographical and climatic parameters that will allow comparison between these two cities.

Parameters	Ibarra	Bogota
Weather	Average of 15.9 ºC	Average of 14.5 ºC
Population	139.721	7,413 millons
Altitude	2215 mamsl	2625 mamsl
Zone	Urban	Urban
Precipitation level	High level of precipitation: February to May and October to November Low level of precipitation: January, June, July, August and September.	High level of precipitation: February to May and October to November Low level of precipitation: January, June, July and August
Contamination Source	Vehicular traffic, emissions of gasoline and diesel from vehicles, sources of combustion, industrial sources, forest fires, soil erosion and construction activities	Vehicular traffic, emissions of gasoline and diesel from vehicles, sources of combustion, industrial sources, forest fires, soil erosion and construction activities

Table 8. Comparation of parameters between Ibarra and Bogota.

As shown in section 4.6 of Bogotá, a study determined a high presence of Al elements. Si, Ca, Fe and K. In the Ibarra graphs presented in the results, high concentration peaks of these elements can also be seen. These traces determined in both Ibarra and Bogotá would be associated with the same sources of pollution associated with the presence of mineral elements and vehicle emissions. These main sources of contamination have been detected in both Ibarra and Bogotá.

9 CONCLUSIONS

Ibarra, San Antonio and Yachay all belonging to the province of Imbabura were chosen to be able to determine the levels of anion cations and elemental trace, taking into account their natural environment location and activities that are carried out in the three different sites. Ibarra considered as a rural area with a greater population than the three cities. Yachay as a developing city and San Antonio as a poorly anthropized area. To determine the concentration levels, rainwater samples were collected each month during a year November 2018 - October 2019. Although the analysis of the last 4 months could not be completed, a total of 36 water samples were collected, 12 samples per each site. From these samples, it was possible to collect soluble material in the water samples and insoluble material in filters.

The analysis of the filters were carried out using X-Ray Fluorescence By Dispersive Energy and for the analysis of water sample three experimental techniques were applied, anions by ion chromatography, cations by means of a continuous flow analyzer and the metal traces by atomic emission spectrometry of inductively coupled plasma. At the same time pH and conductivity values were evaluated.

When analyzing the filters of the three places, it can be concluded that there is a higher concentration (Al, Si, Ca, Fe) and (P, K, Ti, Na, Mg). This elementary trace showed variations in the concentration values in the three sites. The presence of these elements suggests the presence of sources of pollution such as vehicular emissions and the presence of oxides that would be generated by the construction processes, use of soil cement particles. It could also be concluded that the deposition flow increases for (Al, Si, Ca, Fe) throughout the recollection time.

pH values performed on the water samples led to the conclusion that the higher the concentration of (HCO_3^-, SO_4^{2-} and NO_3^-) pH decreases. That said no values were found below 5.6 that would indicate the presence of acid rain.

The conductivity results show slightly higher values in the city of Ibarra, which would indicate a greater presence of ions in that city. These conductivity values are not in the range allowed to be considered drinking water.

Also, from water samples, a high concentration of elemental trace of (Al, Ba, Cu, Cd, Fe, V and Z) and ion concentration (Mg^{2+}, K^+, HCO_3^-, and SO_4^{2-}) were determined. These would be associated with the presence of combustion processes, construction processes specifically the use of cement and production of ceramics and derivatives. Presence of Cl^- and Na^+ would be associated with the influenced of air masses of marine aerosols from the Pacific Ocean. It could also be concluded that the presence of Zn and HCO_3^- as the most abundant in the recollecting time.

To conclude, a study in Bogotá, determined a high concentration of the elements (Al. Si, Ca, Fe and K) which compared to the data obtained experimentally also showed a high concentration of these elements especially in Ibarra and Yachay. Which would confirm a greater presence of these elements in urban than in rural sectors.

10 RECOMMENDATIONS

Complete the experimental analysis of the rain samples from the last four months corresponding to the month of July, August, September and October to have a better picture of the state of contamination.

Complete the experimental analysis with SEM to have a better perspective on the size of particles that are collected in the rainwater samples.

Bibliography

(1) Salud de Nuestro Planeta. Atmosfera https://saluddelplanetatierra.weebly.com/la-atmosfera.html (accessed Jan 7, 2020).

(2) Capas de la tierra. Troposfera - Qué es, Características, Composición, Función y Más https://www.capasdelatierra.org/troposfera/ (accessed Jan 7, 2020).

(3) Lopez, D. Teisserenc de Bort y La esfera de las capas https://www.tutiempo.net/meteorologia/articulos/teisserenc-de-bort.html (accessed Jan 7, 2020).

(4) Rao, P. S. P.; Tiwari, S.; Matwale, J. L.; Pervez, S.; Tunved, P.; Safai, P. D.; Srivastava, A. K.; Bisht, D. S.; Singh, S.; Hopke, P. K. Sources of Chemical Species in Rainwater during Monsoon and Non-Monsoonal Periods over Two Mega Cities in India and Dominant Source Region of Secondary Aerosols. *Atmos. Environ.* **2016**.

(5) Allen, B. Atmospheric Aerosols: What Are They, and Why Are They So Important? **2015**.

(6) Ryan, S.; Leif, J. Aerosoles atmosféricos: una visión general | Temas de ScienceDirect https://www.sciencedirect.com/topics/materials-science/atmospheric-aerosols (accessed Jan 7, 2020).

(7) Gieré, R.; Querol, X. Solid Particulate Matter in the Atmosphere. *Elements* **2010**, *6* (4), 215–222.

(8) Facchini Cerqueira, M. R.; Pinto, M. F.; Derossi, I. N.; Esteves, W. T.; Rachid Santos, M. D.; Costa Matos, M. A.; Lowinsohn, D.; Matos, R. C. Chemical Characteristics of Rainwater at a Southeastern Site of Brazil. *Atmos. Pollut. Res.*

2014, *5* (2), 253–261.

(9) Pöschl, U. Atmospheric Aerosols: Composition, Transformation, Climate and Health Effects. *Angewandte Chemie - International Edition*. November 25, 2005, pp 7520–7540.

(10) Secretaría de Medio Ambiente y Recursos Naturales; Instituto Nacional de Ecología. *Guía Metodológica Para La Estimación de Emisiones de PM 2.5*; 2011.

(11) Marcela Arellano Johnson Waldo Quiroz Vargas Cristian Merino Rubilar Nicole Nilo Olivares Profesora de Química David Vargas Valencia Profesor de Química Sergio Bernal Ramírez Profesor de Química, M. *Propiedades Físico Químcias Del Carbono Equipo de Desarrollo de Contenidos*.

(12) Sosa, G. Elemental carbon and Black carbon https://www.researchgate.net/post/Can_anyone_explain_how_to_distinguish_between_elemental_carbon_and_black_carbon_in_the_atmosphere2 (accessed Jan 12, 2020).

(13) Kulshrestha, U. Assessment of Atmospheric Emissions and Depositions of Major Nr Species in Indian Region. In *The Indian Nitrogen Assessment: Sources of Reactive Nitrogen, Environmental and Climate Effects, Management Options, and Policies*; Elsevier, 2017; pp 427–444.

(14) Aphu Elvis Selase; Danso Eunice Eyra Agyimpomaa; David Deborah Selasi; Dzameh Melody Nina Hakii. Precipitation and Rainfall Types with Their Characteristic Features https://www.researchgate.net/publication/322924903_Precipitation_and_Rainfall_Types_with_Their_Characteristic_Features (accessed Jan 6, 2020).

(15) Instituto Nacional de Meteorologia e Hidrologia. *Republica Del Ecuador Instituto Nacional De Meteorologia E Hidrologia Anuario Meteorológico*; 2017.

(16) Singh, A.; Madhoolike, A. Acid Rain and its ecological consequences https://www.researchgate.net/publication/23295957_Acid_rain_and_its_ecological_consequences (accessed Jan 7, 2020).

(17) Granados Sánchez, D.; López Ríos, G. F.; Hernández García, M. Á. La Lluvia Ácida Y Los Ecosistemas Forestales. *Rev. CHAPINGO Ser. CIENCIAS For. Y DEL Ambient.* **2010**, *XVI* (2), 187–206.

(18) Murrillo, J.; Rodriguez Susana. Determinación de la concentración de aniones en muestras de precipitación total colectadas en San José, Costa Rica. Primera parte http://www.scielo.org.mx/scielo.php?script=sci_arttext&pid=S0188-49992009000200001 (accessed Jan 7, 2020).

(19) HORIBA. Iones en agua y conductividad - LAQUA https://www.horiba.com/us/en/application/material-property-characterization/water-analysis/water-quality-electrochemistry-instrumentation/the-story-of-ph-and-water-quality/the-basis-of-conductivity/ions-in-water-and-conductivity/ (accessed Jan 7, 2020).

(20) Simbaña Karina J. Determinación de Los Niveles de pH, Conductividad, Sulfatos Y Nitratos En Muestras de Agua Lluvia, Recolectadas En Sectores de Alta, Mediana Y Baja Contaminación Ambiental Atmosférica Del Distrito Metropolitano de Quito, 2011.

(21) Lenntech. Conductividad del agua - Lenntech https://www.lenntech.com/applications/ultrapure/conductivity/water-

conductivity.htm (accessed Jan 17, 2020).

(22) Ren-Jian, Z.; Kin-Fai, H.; Zhen-Xing, S. The Role of Aerosol in Climate Change, the Environment, and Human Health. *Atmos. Ocean. Sci. Lett.* **2015**, *5* (2), 156–161.

(23) Lohmann, U.; Feichter, J. Global Indirect Aerosol Effects: A Review. *Atmos. Chem. Phys. Discuss.* **2010**, *4* (6), 7561–7614.

(24) Proctor, J.; Hsiang, S.; Burney, J.; Burke, M.; Schlenker, W. Estimating Global Agricultural Effects of Geoengineering Using Volcanic Eruptions. *Nature*. Nature Publishing Group August 23, 2018, pp 480–483.

(25) Sistema Nacional de Información Ambiental y de Recursos Naturales. Informe del Medio Ambiente https://apps1.semarnat.gob.mx:8443/dgeia/informe15/tema/cap5.html (accessed Jan 17, 2020).

(26) Organizacion Mundial de la Salud. Calidad del aire ambiente (exterior) y salud https://www.who.int/es/news-room/fact-sheets/detail/ambient-(outdoor)-air-quality-and-health (accessed Jan 7, 2020).

(27) Ecologistas en accion. La calidad del aire en el Estado español durante 2010 https://www.ecologistasenaccion.org/wp-content/uploads/adjuntos-spip/pdf/informe_calidad_aire_2011.pdf (accessed Jan 7, 2020).

(28) Oyarzún, M. Contaminación aérea y sus efectos en la salud* https://scielo.conicyt.cl/pdf/rcher/v26n1/art04.pdf (accessed Jan 12, 2020).

(29) Sostenibilidad. Los efectos de la contaminación atmosférica sobre la salud https://www.sostenibilidad.com/medio-ambiente/efectos-contaminacion-

atmosferica-salud/ (accessed Jan 12, 2020).

(30) Riojas, H.; Pamela, M. C.; Zúñiga Bello, E. *Dia Interamericano De Calidad Del Aire*; 2017.

(31) Martinez, E. *Química*; Cengage Learning, Ed.

(32) Sagu, X. Causas naturales de la contaminación del aire: incendios forestales | AirGO https://www.airgo2.com/air-pollution/causes/natural/forest-fire/#targetText=Particulates on forest fire are,penetrate deeply into humans lungs. (accessed Jan 7, 2020).

(33) Servicio Nacional De Gestion de Riesgos y Emergencias. *Incendios Forestales a Nivel Nacional 2019*; 2019.

(34) McGonigle, A. J. S.; Oppenheimer, C. Optical Sensing of Volcanic Gas and Aerosol Emissions. *Geol. Soc. London, Spec. Publ.* **2003**, *213* (1), 149–168.

(35) Instituto Geofísico - EPN. Informe Diario Reventador https://www.igepn.edu.ec/reventador-informes/rev-diarios/rev-d-2019/22950-informe-diario-reventador-04-09-2019 (accessed Jan 7, 2020).

(36) Business School. ¿Qué características tiene un proceso industrial? | OBS Business School https://obsbusiness.school/int/blog-project-management/proyectos-de-ingenieria/que-caracteristicas-tiene-un-proceso-industrial (accessed Jan 12, 2020).

(37) Ministerio para la Transportación Ecológica. Sector del refino https://www.miteco.gob.es/es/calidad-y-evaluacion-ambiental/temas/atmosfera-y-calidad-del-aire/emisiones/act-emis/otras_instalaciones_industriales.aspx (accessed Jan 7, 2020).

(38) RK Gupta; JV Trivedi; Deepanjan Majumdar; AD Bhanarkar. (PDF) Particulate Matter and Elemental Emissions from a Cement Kiln. **2012**, 1–9.

(39) Google Maps https://www.google.com/maps/@0.3392909,-78.2221886,15z (accessed Jan 7, 2020).

(40) Facultad de Agronomía | Universidad de Buenos Aires. *Contaminación Atmosférica*.

(41) Rönkkö, T.; Kuuluvainen, H.; Karjalainen, P.; Keskinen, J.; Hillamo, R.; Niemi, J. V.; Pirjola, L.; Timonen, H. J.; Saarikoski, S.; Saukko, E.; Järvinen, A.; Silvennoinen, H.; Rostedt, A.; Olin, M.; Yli-Ojanperä, J.; Nousiainen, P.; Kousa, A.; Dal Maso, M. Traffic Is a Major Source of Atmospheric Nanocluster Aerosol. *Proc. Natl. Acad. Sci. U. S. A.* **2017**, *114* (29), 7549–7554.

(42) Illicachi, A. La Contaminación Del Medio Ambiente Provocado Por Los Vehículos a Motor Por La Emisión de Monóxido de Carbono Y Su Incidencia En La Salud de La Población Del Centro Histórico de Quito En El Año 2014, 2015.

(43) Redaccion Sociedad. El transporte motorizado es el que más contamina https://www.eltelegrafo.com.ec/noticias/sociedad/6/transporte-motorizado-contaminacion-ambiental-ecuador (accessed Jan 7, 2020).

(44) Sanderson, P.; Su, S. S.; Chang, I. T. H.; Delgado Saborit, J. M.; Kepaptsoglou, D. M.; Weber, R. J. M.; Harrison, R. M. Characterisation of Iron-Rich Atmospheric Submicrometre Particles in the Roadside Environment. *Atmos. Environ.* **2016**, *140*, 167–175.

(45) College of Engineering Pennstate. Composition of cement https://www.engr.psu.edu/ce/courses/ce584/concrete/library/construction/curing/

composition of cement.htm (accessed Jan 24, 2020).

(46) Laboratorio y Servicios Agropecuarios. Composición Química De Fertilizantes www.laboratoriomarasas.com.ar (accessed Jan 24, 2020).

(47) (PDF) Contaminación por fósforo procedente de la fertilización orgánica de suelos agrícolas https://www.researchgate.net/publication/230688083_Contaminacion_por_fosforo_procedente_de_la_fertilizacion_organica_de_suelos_agricolas (accessed Jan 7, 2020).

(48) Perú Ecológico. El ciclo del potasio https://www.peruecologico.com.pe/lib_c2_t13.htm (accessed Jan 11, 2020).

(49) Agency for Toxic Substance Disease Registry. ATSDR - ToxFAQs™: Barium https://www.atsdr.cdc.gov/toxfaqs/tf.asp?id=326&tid=57 (accessed Jan 7, 2020).

(50) Atsdr. Toxicological Profile For Cadmium https://www.atsdr.cdc.gov/toxprofiles/tp5.pdf (accessed Jan 7, 2020).

(51) Atsdr. Toxicological Profile for Vanadium https://www.atsdr.cdc.gov/toxprofiles/tp58.pdf (accessed Jan 7, 2020).

(52) Atsdr. Toxicological Profile For Zinc https://www.atsdr.cdc.gov/ToxProfiles/tp60.pdf (accessed Jan 7, 2020).

(53) Parnes, R. Magnesium https://www.nofa.org/soil/html/magnesium.php (accessed Jan 11, 2020).

(54) Atsdr. Toxicological Profile For Copper https://www.atsdr.cdc.gov/ToxProfiles/tp132.pdf (accessed Jan 7, 2020).

(55) Centro Iberoamericano de Desarrollo Estratégico Urbano. Bogotá | Descripción https://www.cideu.org/miembro/bogota/ (accessed Jan 20, 2020).

(56) Secretaria Distrital de Ambiente. Informe anual calidad del aire Bogotá 2018 – Observatorio Ambiental de Bogota http://oab.ambientebogota.gov.co/?post_type=dlm_download&p=13003 (accessed Jan 10, 2020).

(57) Ramírez, O.; Sánchez de la Campa, A. M.; Amato, F.; Catacolí, R. A.; Rojas, N. Y.; de la Rosa, J. Chemical Composition and Source Apportionment of PM10 at an Urban Background Site in a High–altitude Latin American Megacity (Bogota, Colombia). *Environ. Pollut.* **2018**, *233*, 142–155.

(58) Ibarra, Ciudad blanca a la que siempre se vuelve https://www.ibarra.gob.ec/site/ (accessed Jan 7, 2020).

(59) Ministerio del Ambiente. Inventario Preliminar de Las Emisiones de Contaminantes Del Aire, de Los Cantones Ambato, Riobamba, Santo Domingo de Los Colorados, Latacunga, Ibarra, Manta, Portoviejo, Esmeraldas Y Milagro. **2010**, 28.

(60) Gad San Antonio de Ibarra. San Antonio de Ibarra http://www.gadsanantonioibarra.gob.ec/inicio/index.php/en/gad/2016-10-05-16-24-39 (accessed Jan 10, 2020).

(61) Ubicación Geográfica – GAD Municipal de San Miguel de Urcuquí https://www.urcuqui.gob.ec/ubicacion-geografica/ (accessed Jan 7, 2020).

(62) De, F.; Cruz, L. A.; Lima, E. *Fluorescencia de Rayos X Y Su Aplicación En La Determinación de Elementos Químicos En Determinadas Muestras*; 2018.

(63) Ferrero, J. L.; Roldán, C.; Juanes, D.; Lluch, J. L.; Ardid, M. *Evolución De La Instrumentación De Fluorescencia De Rayos-X En La Unidad De Arqueometría Del Icmuv.*

(64) Malvern Panalytical. Energy Dispersive Spectroscopy | EDXRF Spectrometers | EDX Analysis https://www.malvernpanalytical.com/en/products/technology/x-ray-fluorescence/energy-dispersive-x-ray-fluorescence (accessed Jan 10, 2020).

(65) EAG Laboratories. Cromatografía de iones | IC | Análisis de Iones | Laboratorios EAG https://www.eag.com/es/techniques/chromatography/ion-chromatography-ic/ (accessed Jan 23, 2020).

(66) 881 Compact IC pro – Anion https://www.metrohm.com/es/productos/28810020 (accessed Jan 23, 2020).

(67) Editors, L. Continuous Flow Analysis & Discrete Analyzers.

(68) Ruzicka, J. (Jarda). From Continuous Flow Analysis to Programmable Flow Injection Techniques. A History and Tutorial of Emerging Methodologies. *Talanta*. Elsevier B.V. 2016, pp 299–305.

(69) Espectroscopía De Emisión Por Plasma De Acoplamiento Inductivo. https://sstti.ua.es/es/instrumentacion-cientifica/unidad-de-analisis/espectroscopia-de-emision-por-plasma-de-acoplamiento-inductivo.html (accessed Jan 23, 2020).

(70) Rutzke, M. A. Atomic Absorption, Inductively Coupled Plasma Optical Emission Spectroscopy, and Infrared Spectroscopy. In *Encyclopedia of Earth Sciences Series*; Springer Netherlands, 2018; pp 76–83.

(71) NOAA HYSPLIT Trajectory Model https://www.ready.noaa.gov/hypub-bin/trajresults.pl?jobidno=13931 (accessed Jan 7, 2020).

Annexes

FECHA	Nombre Muestra (	Be (µg/L)	Cd (µg/L)	Co (µg/L)	Cr (µg/L)	Cu (µg/L)	Fe (µg/L)	Hg (µg/L)	Mn (µg/L)	Mo (µg/L)	Ni (µg/L)	Pb (µg/L)	Sb (µg/L)	Se (µg/L)	Th (µg/L)	Tl (µg/L)	U (µg/L)	V (µg/L)	Zn (µg/L)
09/08/2019	Yachay-1	< 0,05	0,71	0,01	< 0,05	0,61	0,17	< 0,5	< 0,5	0,38	< 0,5	< 0,2	0,09	< 0,5	< 0,05	< 0,05	< 0,05	0,12	8,13
09/08/2019	Yachay-2	< 0,05	0,61	0	0,06	1,8	0,16	< 0,5	0,52	< 0,2	0,52	< 0,2	0,38	< 0,5	< 0,05	< 0,05	< 0,05	0,62	6,95
09/08/2019	Yachay-3	< 0,05	0,72	0,02	0,05	0,66	0,17	< 0,5	0,86	0,28	< 0,5	< 0,2	0,09	< 0,5	< 0,05	< 0,05	< 0,05	0,18	13,9
09/08/2019	Yachay-4	< 0,05	1,12	0,02	0,11	0,93	1,98	< 0,5	1,22	0,31	< 0,5	< 0,2	0,05	< 0,5	< 0,05	< 0,05	< 0,05	0,12	22,1
09/08/2019	Yachay-5	< 0,05	0,36	0,01	< 0,05	0,88	0,29	< 0,5	< 0,5	< 0,2	< 0,5	< 0,2	0,05	< 0,5	< 0,05	< 0,05	< 0,05	0,32	18,4
09/08/2019	Yachay-6	< 0,05	0,52	0,04	< 0,05	1,89	0,32	< 0,5	1,98	< 0,2	< 0,5	< 0,2	0,07	< 0,5	< 0,05	< 0,05	< 0,05	0,12	11,8
09/08/2019	Yachay-7	< 0,05	0,47	0,01	< 0,05	0,37	0,19	< 0,5	< 0,5	< 0,2	< 0,5	< 0,2	< 0,05	< 0,5	< 0,05	< 0,05	< 0,05	0,11	7,72
09/08/2019	Yachay-8	< 0,05	0,83	0,02	0,05	7,64	2,06	< 0,5	< 0,5	0,22	< 0,5	< 0,2	0,22	< 0,5	< 0,05	< 0,05	< 0,05	0,82	29,8
09/08/2019	Ibarra-1	< 0,05	0,48	0	< 0,05	0,52	0,11	< 0,5	< 0,5	< 0,2	< 0,5	< 0,2	0,11	< 0,5	< 0,05	< 0,05	< 0,05	0,1	8,64
09/08/2019	Ibarra-2	< 0,05	0,36	0,01	0,31	2,48	0,7	< 0,5	< 0,5	0,24	< 0,5	< 0,2	0,84	< 0,5	< 0,05	< 0,05	< 0,05	0,97	6,97
09/08/2019	Ibarra-3	< 0,05	0,8	0,01	0,22	1,2	0,51	< 0,5	< 0,5	0,2	< 0,5	< 0,2	0,18	< 0,5	< 0,05	< 0,05	< 0,05	0,26	21
09/08/2019	Ibarra-4	< 0,05	0,5	0,02	< 0,05	1,49	0,07	< 0,5	0,56	< 0,2	< 0,5	< 0,2	< 0,05	< 0,5	< 0,05	< 0,05	< 0,05	0,16	10
09/08/2019	Ibarra-5	< 0,05	0,43	0,09	0,15	2,48	1,48	< 0,5	< 0,5	0,2	< 0,5	< 0,2	0,07	< 0,5	< 0,05	< 0,05	< 0,05	3,73	9,28
09/08/2019	Ibarra-6	< 0,05	0,43	< 0,05	< 0,05	0,38	2,05	< 0,5	1,59	< 0,2	< 0,5	< 0,2	0,08	< 0,5	< 0,05	< 0,05	< 0,05	0,11	17,8
09/08/2019	Ibarra-7	< 0,05	0,45	< 0,05	0,1	0,37	0,59	< 0,5	< 0,5	< 0,2	< 0,5	< 0,2	0,07	< 0,5	< 0,05	< 0,05	< 0,05	0,11	12,3
09/08/2019	Ibarra-8	< 0,05	0,39	< 0,05	0,07	1,3	0,12	< 0,5	< 0,5	0,3	< 0,5	< 0,2	0,21	< 0,5	< 0,05	< 0,05	< 0,05	0,35	20,2
09/08/2019	San Antonio-1	< 0,05	0,43	< 0,05	< 0,05	0,49	1,17	< 0,5	< 0,5	0,26	< 0,5	< 0,2	0,24	< 0,5	< 0,05	< 0,05	< 0,05	0,09	10
09/08/2019	San Antonio-2	< 0,05	0,4	< 0,05	< 0,05	2,16	3,32	< 0,5	1,11	< 0,2	< 0,5	< 0,2	0,33	< 0,5	< 0,05	< 0,05	< 0,05	0,12	11,4
09/08/2019	San Antonio-3	< 0,05	0,44	< 0,05	< 0,05	0,56	1,39	< 0,5	0,68	0,34	< 0,5	< 0,2	0,14	< 0,5	< 0,05	< 0,05	< 0,05	0,05	8,51
09/08/2019	San Antonio-6	< 0,05	0,42	< 0,05	0,3	0,36	1,58	< 0,5	0,67	< 0,2	< 0,5	< 0,2	< 0,05	< 0,5	< 0,05	< 0,05	< 0,05	0,08	20,8
09/08/2019	San Antonio-7	< 0,05	0,44	0,05	< 0,05	0,84	0,53	< 0,5	1,08	0,26	0,62	< 0,2	< 0,05	< 0,5	< 0,05	< 0,05	< 0,05	0,06	19,5
09/08/2019	San Antonio-8	< 0,05	0,21	< 0,05	0,33	1,47	0,93	< 0,5	0,74	< 0,2	< 0,5	< 0,2	< 0,05	< 0,5	< 0,05	< 0,05	< 0,05	0,15	24,1

Figure 39. Results of experimental data of elemental trace and ions of rainwater samples.

Area muestreada		12,5664						
Masa filtro	*24,7*	*4,6*	*14*	*10,3*	*10,5*	*1,6*	*6,9*	*12,5*
Masa total	***35,2***	***4,6***	***42,2***	***20,6***	***34,8***	***6,2***	***12,6***	***12,5***
	IBARRA1.2	IBARRA2.1	IBARRA3.1	IBARRA4.1	Ibarra5.1	Ibarra6.1	Ibarra7.1	Ibarra8.1
Na	4,322	1,521	2,491	2,28	1,589	0,974	0,993	2,337
Mg	2,842	0,89	1,409	1,207	1,295	0,534	0,524	1,295
Al	22,49	6,198	10,073	9,185	4,396	2,735	3,584	9,153
Si	16,781	6,685	13,576	12,162	14,504	5,572	9,834	14,474
P	0,783	0,688	1,077	0,815	1,358	0,556	0,601	1,965
S	0,977	0,4838	1,299	1,362	1,738	0,5464	0,8162	1,195
Cl	0,5333	0,1125	0,2026	0,1476	0,0946	0,0865	0,0869	0,1693
K	7,413	2,0034	4,653	4,247	3,4926	1,5076	1,7769	3,797
Ca	25,562	5,554	8,626	7,035	4,943	2,1729	2,9142	10,207
Sc	0,1053							
Ti	4,151	0,632	1,302	1,108	0,535	0,372	0,468	1,195
V	0,162	0,0208	0,0267	0,038	0,0203	0,014		0,044
Cr	0,0812	0,009	0,0098	0,0139				0,0097
Mn	0,8645	0,1487	0,2454	0,1812	0,1165	0,0354	0,062	0,2498
Fe	52,839	7,173	11,742	9,965	5,122	2,2425	3,249	13,284
Ni								
Cu	0,2807	0,0713	0,1288	0,1047	0,1295	0,0572	0,0529	0,0713
Zn	0,7326	0,1736	0,2751	0,2438	0,2752	0,1165	0,1697	0,3145
Ge							0,0058	
As	0,0328			0,0079				
Se								
Br	0,0138	0,0068		0,0057		0,007		0,0075
Rb	0,0721	0,0123	0,0153	0,0185	0,0194	0,0056	0,0059	0,0162
Sr	0,9624	0,1878	0,2209	0,2053	0,1064	0,0534	0,0658	0,2877
Y	0,0173	0,0071	0,0089	0,011				0,013
Nb								
Mo								
Ag				0,441		0,088		
Te				0				
Ba	0,763	0,267	0,275	0,234	0,114	0,075	0,145	0,236
W	0,0486	0,0273	0,0567	0,0381	0,0495	0,0396	0,0598	0,0365
Pb	0,0261	0,0147	0,0173	0,0163	0,0117	0,0082	0,0149	0,0211
Bi								

Figure 40. Results of experimental data of the filters obtained from the samples of the rainwater samples in Ibarra.

Area muestreada													
Masa filtro	*3,3*	*2,8*	*2,9*	*4,3*	*6,1*	*8,6*	*63,4*	*0,7*	*4,6*	*21,7*	*8,6*	*6*	*3,1*
Masa total	***24,8***	***3,2***	***19,5***	***13***	***17,3***	***8,6***	***73***	***0,7***	***15,6***	***40***	***8,6***	***6***	***3,1***
	San Antonio 1.1	San Antonio 2.1	San Antonio 3.1	San Antonio 6.1	San Antonio 7.2	San Antonio 8.1	Yachay 1.2	Yachay 2.1	Yachay 3.1	Yachay 4.3	Yachay 5.1	Yachay 6.1	Yachay 8.1
Na	0,477	0,533	0,557	0,804	1,277	1,55	4,09	0,729	0,558	5,772	3,947	2,787	0,938
Mg	0,536	0,427	0,369	0,43	0,649	0,848	2,506	0,526	0,417	3,281	2,259	1,351	0,638
Al	0,671	1,318	1,189	1,238	2,271	4,214	21,61	2,743	2,665	27,67	19,96	11,363	3,948
Si	5,856	6,779	5,32	6,542	9,51	10,994	20,593	3,204	6,474	16,934	11,349	9,931	6,494
P	1,708	1,191	1,179	1,728	2,798	2,68	0,554	0,636	0,71	0,543	0,431	0,455	1,339
S	1,1125	0,9372	0,7524	1,0497	1,637	1,715	0,634	0,3379	0,7821	0,72	0,436	0,5912	0,4766
Cl	0,0548	0,0965	0,0301	0,0719	0,1006	0,0597	0,1188	0,0986	0,3345	0,2236	0,1302	0,4299	0,0623
K	1,6053	1,1098	0,9802	2,7965	3,3077	1,7811	9,481	1,1113	0,8965	10,168	6,505	3,599	1,5101
Ca	2,0643	1,5175	1,0975	0,9784	1,9822	4,946	22,084	1,5922	1,556	20,908	12,761	7,583	3,0525
Sc							0,1379			0,0952	0,0371		
Ti	0,0563	0,1413	0,0787	0,1174	0,1919	0,459	4,45	0,1992	0,2449	3,536	2,032	1,182	0,3488
V		0,0127		0	0	0,0166	0,261			0,139	0,065	0,0294	0,0124
Cr					0,0216	0,0159	0,0718			0,0507	0,0277		
Mn	0,0521	0,0356	0,0321	0,0303	0,0501	0,1424	1,244	0,059	0,1162	0,7033	0,4242	0,1794	0,0883
Fe	0,6912	1,4392	1,0352	1,3492	2,1779	5,432	69,58	2,4399	2,966	44,626	24,18	12,256	4,393
Ni						0,0109	0,0207						
Cu	0,0281	0,0343	0,0376	0,0231	0,0461	0,0539	0,2698	0,0352	0,0818	0,2344	0,0702	0,1085	0,0408
Zn	0,1298	0,0918	0,0806	0,6183	1,3478	1,993	0,5603	0,0953	0,1138	0,2823	0,2251	0,1726	0,1323
Ge				0,0076	0,0098	0,0091							
As							0,0388			0,0181	0,0092	0,0045	
Se													
Br		0,0098	0,0069	0,0067	0,0057	0,0049	0,0127		0,0059	0,0125	0,0057	0,0066	
Rb					0,0098	0,0052	0,1445	0,0058	0,0062	0,0826	0,0399	0,0199	0,0064
Sr	0,0161	0,0252	0,024	0,0251	0,0486	0,1116	1,3838	0,039	0,0343	0,8354	0,3632	0,2289	0,0751
Y				0,0066	0,0062		0,0253			0,0149	0,0091	0,0071	
Nb							0,03						
Mo												0,51	
Ag				0,781	0,423							0,135	
Te	0	0		0			0	0			0		
Ba	0,068	0,048	0,0474	0,041	0,064	0,13	1,121	0,078	0,058	0,831	0,424	0,263	0,095
W	0,0315	0,0238	0,0298	0,0742	0,096	0,1043	0,0546	0,0375	0,0195	0,0233	0,0171	0,0231	0,0294
Pb			0,01	0,009	0,011	0,0141			0,0084			0,0111	0,0141
Bi			0,0053										0,0061

Figure 41. Results of experimental data of the filters obtained from the samples of the rainwater samples in San Antonio and Yachay.